Courant-sharp eigenvalues for the equilateral torus, and for the equilateral triangle

Pierre Bérard, Bernard Helffer

Courant-sharp eigenvalues for the equilateral torus, and for the equilateral triangle

P. Bérard
Institut Fourier, Université de Grenoble and CNRS, B.P.74,
F 38402 Saint Martin d'Hères Cedex, France.
and
B. Helffer
Laboratoire de Mathématiques, Univ. Paris-Sud 11 and CNRS,
F 91405 Orsay Cedex, France, and
Laboratoire Jean Leray, Université de Nantes.

March 11, 2015

Abstract

We address the question of determining the eigenvalues λ_n (listed in nondecreasing order, with multiplicities) for which Courant's nodal domain theorem is sharp i.e., for which there exists an associated eigenfunction with n nodal domains (Courant-sharp eigenvalues). Following ideas going back to Pleijel (1956), we prove that the only Courant-sharp eigenvalues of the flat equilateral torus are the first and second, and that the only Courant-sharp Dirichlet eigenvalues of the equilateral triangle are the first, second, and fourth eigenvalues. In the last section we sketch similar results for the right-angled isosceles triangle and for the hemiequilateral triangle.

Keywords: Nodal lines, Nodal domains, Courant theorem.
MSC 2010: 35B05, 35P20, 58J50.

1 Introduction

Let (M, g) be a compact Riemannian manifold, and Δ the nonpositive Laplace-Beltrami operator. Consider the eigenvalue problem $-\Delta u = \lambda u$, with Dirichlet boundary condition in case M has a boundary. Write the eigenvalues in nondecreasing order, with multiplicities,

$$\lambda_1(M) < \lambda_2(M) \leq \lambda_3(M) \leq \cdots .$$

Courant's theorem [7] states that an eigenfunction u, associated with the k-th eigenvalue λ_k, has at most k nodal domains. We say that λ_k is *Courant-sharp* if there exists an eigenfunction u, associated with λ_k, with exactly k nodal domains. Pleijel [18] (see also [5]) has shown that the only Dirichlet eigenvalues of a square which are Courant-sharp are the first, second and fourth eigenvalues. Léna [14] recently proved that the only Courant-sharp eigenvalues of the square flat torus are the first and second eigenvalues.

In this paper, following [18] and [14], we determine the Courant sharp eigenvalues for the equilateral torus and the equilateral triangle (with Dirichlet boundary condition).

Theorem 1.1 *The only Courant-sharp eigenvalues of the equilateral torus are the first and second eigenvalues.*

Theorem 1.2 *The only Courant sharp eigenvalues of the equilateral triangle are the first, second, and fourth eigenvalues.*

The Dirichlet eigenvalues and eigenfunctions of the equilateral triangle were originally studied by Lamé [13], and later in the papers [16, 2, 17]. We refer to [15] for a detailed account, and to [12, §6] for another approach.

In [2], the author determined the Dirichlet and Neumann eigenvalues and eigenfunctions for the fundamental domains of crystallographic groups, namely the fundamental domains (or *alcoves*) of the action of the affine Weyl group W_a generated by the reflections associated with a root system [6]. In the two-dimensional case, the domains are the rectangle, the equilateral triangle, the right isosceles triangle, and the triangle with angles $(30, 60, 90)$ degrees. The same ideas [3] can be applied to determine the Dirichlet and Neumann eigenvalues of the spherical domains obtained as intersections of the round sphere with the fundamental domain (or *chamber*) of the Weyl group W associated with a root system.

In Section 2, we describe the proper geometric framework to determine the eigenvalues of the equilateral triangle, following the ideas of [2], but without references to root systems. For the convenience of the reader, we use the same notation as in [6, 2].

In Section 3, following [14], we study the Courant-sharp eigenvalues of the equilateral torus, and prove Theorem 1.1.

Starting from Section 4, we describe the spectrum of the equilateral triangle, and the symmetries of the eigenfunctions. In Section 5, following Pleijel's approach [18], we reduce the question of Courant-sharp eigenvalues to the analysis of only two eigenspaces associated with the eigenvalues λ_5 and λ_7, which are studied in Sections 7 and 8 respectively after a presentation of the strategy in Section 6.

In Section 10, we sketch similar results for the right-angled isosceles triangle and for the hemiequilateral triangle. In both cases, the only Courant-sharp eigenvalues are the first and second.

The authors would like to thank Virginie Bonnaillie-Noël for communicating her numerical computations of eigenvalues and nodal sets for the triangular domains.

2 The geometric framework

We call $\mathbb{E}^2$ the vector (or affine) space $\mathbb{R}^2$ with the canonical basis $\{e_1 = (1,0), e_2 = (0,1)\}$, and with the standard Euclidean inner product $\langle \cdot, \cdot \rangle$ and norm $|\cdot|$.

Define the vectors

$$\alpha_1 = \left(1, -\frac{1}{\sqrt{3}}\right), \ \alpha_2 = \left(0, \frac{2}{\sqrt{3}}\right), \ \text{and } \alpha_3 = \left(1, \frac{1}{\sqrt{3}}\right). \tag{2.1}$$

The vectors α_1, α_2 span $\mathbb{E}^2$. Furthermore, $|\alpha_i| = \frac{2}{\sqrt{3}}$, $\measuredangle(\alpha_1, \alpha_2) = \frac{2\pi}{3}$, and $\measuredangle(\alpha_1, \alpha_3) = \measuredangle(\alpha_3, \alpha_2) = \frac{\pi}{3}$ (here $\measuredangle$ denotes the angle between two vectors).

Introduce the vectors

$$\alpha_i^\vee = \frac{2}{\langle \alpha_i, \alpha_i \rangle} \alpha_i \,, \text{for } i = 1, 2, 3 \,.$$

Then,

$$\alpha_1^\vee = \left(\frac{3}{2}, -\frac{\sqrt{3}}{2}\right), \ \alpha_2^\vee = \left(0, \sqrt{3}\right), \ \text{and } \alpha_3^\vee = \left(\frac{3}{2}, \frac{\sqrt{3}}{2}\right). \tag{2.2}$$

For $i \in \{1, 2, 3\}$, introduce the lines

$$L_i = \left\{ x \in \mathbb{E}^2 \mid \langle x, \alpha_i \rangle = 0 \right\}, \tag{2.3}$$

and the orthogonal symmetries with respect to these lines,

$$s_i(x) = x - \frac{2\langle x, \alpha_i \rangle}{\langle \alpha_i, \alpha_i \rangle} \alpha_i \,. \tag{2.4}$$

Let W be the group generated by the symmetries $\{s_1, s_2, s_3\}$.

More generally, for $i \in \{1, 2, 3\}$ and $k \in \mathbb{Z}$, consider the lines

$$L_{i,k} = \left\{ x \in \mathbb{E}^2 \mid \langle x, \alpha_i \rangle = k \right\}, \tag{2.5}$$

and the orthogonal symmetries with respect to these lines,

$$s_{i,k}(x) = x - \frac{2\langle x, \alpha_i \rangle}{\langle \alpha_i, \alpha_i \rangle} \alpha_i + k\alpha_i^\vee = s_i(x) + k\alpha_i^\vee \,. \tag{2.6}$$

Let W_a be the group generated by the symmetries $\{s_{i,k} \mid i = 1, 2, 3 \text{ and } k \in \mathbb{Z}\}$.

These groups are called respectively the *Weyl group* and the *affine Weyl group* [6].

Call Γ the group generated by $\alpha_1^\vee$ and $\alpha_2^\vee$ (see the notation $Q(R^\vee)$ in [6, 2]) i.e.,

$$\Gamma = \mathbb{Z}\,\alpha_1^\vee \bigoplus \mathbb{Z}\,\alpha_2^\vee \,. \tag{2.7}$$

The following properties are easy to establish (see Figure 2.1).

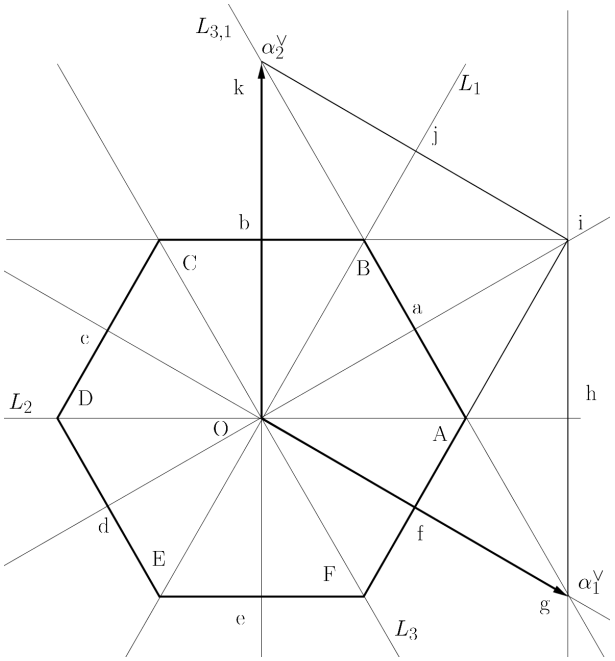

Figure 2.1: The geometric framework

Proposition 2.1 *With the above notation, the following properties hold.*

1. *The group W has six elements; it is isomorphic to the symmetric group in three letters $\mathcal{S}_3$.*

2. *The group W acts simply transitively on the connected components of $\mathbb{E}^2 \setminus L_1 \cup L_2 \cup L_3$ (the Weyl chambers).*

3. *The group W_a is the semi-direct product $\Gamma \rtimes W$. A fundamental domain for the action of W_a on $\mathbb{E}^2$ is the closed equilateral triangle $\mathcal{T}$, with vertices $O = (0,0)$, $A = (1,0)$, and $B = (\frac{1}{2}, \frac{\sqrt{3}}{2})$.*

4. *The group W acts simply transitively on the equilateral triangles which tile the regular hexagon $[A, B, \ldots, E, F]$.*

5. *The closed regular hexagon $[A, B, \ldots, E, F]$ is a fundamental domain for the action of the lattice Γ on $\mathbb{E}^2$.*

Proof.
(1) Clearly, $s_1^2 = 1$ (where 1 is the identity), $s_2^2 = 1$, $s_3^2 = 1$, and $s_3 = s_1 \circ s_2 \circ s_1 = s_2 \circ s_1 \circ s_2$. Furthermore, $s_1 \circ s_2$, $s_3 \circ s_1$ and $s_2 \circ s_3$ are equal to the rotation with center O and angle $\frac{2\pi}{3}$; $s_2 \circ s_1$, $s_1 \circ s_3$ and $s_3 \circ s_2$ are equal to the rotation with center O and angle $-\frac{2\pi}{3}$. It follows that

$$W = \{1, s_1, s_2, s_3, s_1 \circ s_2, s_2 \circ s_1\} .$$

To see that W is isomorphic to $\mathcal{S}_3$, look at its action on the lines $\mathbb{R}\,\alpha_i$, $i = 1, 2, 3$.
(2) Clear.
(3) Write the action of $(\gamma, \sigma) \in \Gamma \times W$ on $\mathbb{E}^2$, as

$$x \mapsto (\gamma, \sigma) \cdot x = \sigma(x) + \gamma .$$

Then, $(\gamma,\sigma).(\gamma',\sigma') = (\gamma+\sigma(\gamma'),\sigma\circ\sigma')$. Clearly, $s_{i,k}$ can be written as $(k\alpha_i^\vee, s_i)$ and hence, $W_a \subset \Gamma \rtimes W$. To prove the reverse inclusion, we first remark that $s_i(\alpha_i^\vee) = -\alpha_i^\vee$, and that $s_1(\alpha_2^\vee) = s_2(\alpha_1^\vee) = \alpha_1^\vee + \alpha_2^\vee$. Note also that for $m,n \in \mathbb{Z}$, we have $s_{i,m}\circ s_{i,n} = \big((m-n)\alpha_i^\vee, 1\big)$. One can then write

$$(m\alpha_1^\vee + n\alpha_2^\vee, s_1) = s_{2,n}\circ s_2 \circ s_{1,m}\,,$$

and

$$(m\alpha_1^\vee + n\alpha_2^\vee, s_2\circ s_1) = s_2 \circ s_{2,m}\circ s_{2,n}\circ s_{1,m}\,,$$

and similar identities to conclude. The fact that the equilateral triangle with vertices $O=(0,0)$, $A=(1,0)$, and $B=(\frac{1}{2},\frac{\sqrt{3}}{2})$ is a fundamental domain for W_a follows from the fact that the sides of the triangle are supported by the lines L_1, L_2 and $L_{3,1}$.
(4) Clear.
(5) This assertion is illustrated by Figure 2.2. More precisely, we have the following correspondences of triangles which move the hexagon onto the fundamental domain $\{x\alpha_1^\vee + y\alpha_1^\vee \mid 0\le x,y\le 1\}$ for the action of Γ on $\mathbb{E}^2$.

Triangle	sent to	by
$[0,b,C]$	$[g,h,A]$	$\alpha_1^\vee$
$[0,C,c]$	$[g,A,f]$	$\alpha_1^\vee$
$[0,c,D]$	$[i,j,B]$	$\alpha_3^\vee$
$[0,D,d]$	$[i,B,a]$	$\alpha_3^\vee$
$[0,d,E]$	$[i,a,A]$	$\alpha_3^\vee$
$[0,E,e]$	$[i,A,h]$	$\alpha_3^\vee$
$[0,e,F]$	$[k,b,B]$	$\alpha_2^\vee$
$[0,F,f]$	$[k,B,j]$	$\alpha_2^\vee$

□

3 The equilateral torus

3.1 Preliminaries

The *equilateral torus* is the flat torus $\mathbb{T} = \mathbb{E}^2/\Gamma$, where Γ is the lattice $\mathbb{Z}\,\alpha_1^\vee \bigoplus \mathbb{Z}\,\alpha_2^\vee$.

Let Γ^* be the dual lattice (see the notation $P(R)$ in [6, 2])

$$\Gamma^* = \big\{x\in\mathbb{E}^2 \mid \langle x,\gamma\rangle \in \mathbb{Z},\ \forall\gamma\in\Gamma\big\}\ . \tag{3.1}$$

The lattice Γ^* admits the basis $\{\varpi_1,\varpi_2\}$, where

$$\varpi_1 = (\frac{2}{3},0),\ \varpi_2 = (\frac{1}{3},\frac{1}{\sqrt{3}}), \tag{3.2}$$

which is dual to the basis $\{\alpha_1^\vee,\alpha_2^\vee\}$ of Γ.

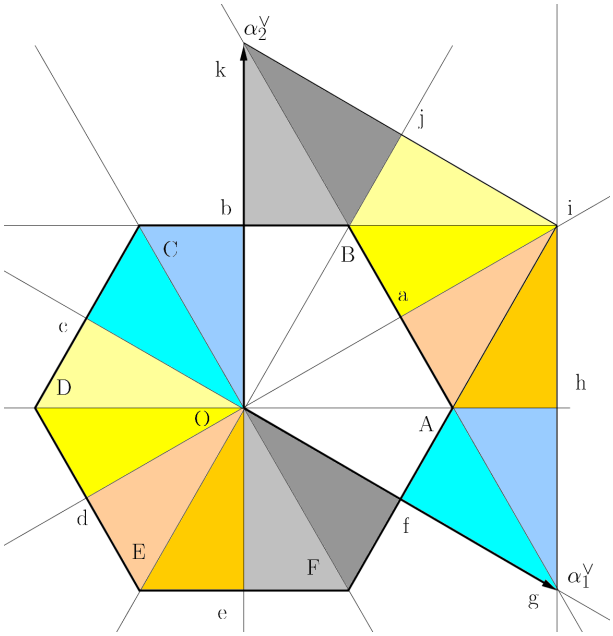

Figure 2.2: The hexagon is a fundamental domain for Γ

Up to normalization, a complete set of eigenfunctions of the torus $\mathbb{T}$ is given by

$$\phi_p(x) = \exp(2i\pi\langle x, p\rangle), \tag{3.3}$$

where p ranges over Γ^*, and $x \in \mathbb{E}^2$. More precisely, for $p \in \Gamma^*$, the function ϕ_p satisfies

$$-\Delta\phi_p = 4\pi^2|p|^2\phi_p.$$

Writing $p = m\varpi_1 + n\varpi_2$, we find that the eigenvalues of the equilateral torus $\mathbb{T}$ are the numbers

$$\hat{\lambda}(m,n) = \frac{16\pi^2}{9}(m^2 + mn + n^2), \text{ for } m, n \in \mathbb{Z}\,. \tag{3.4}$$

The multiplicity of the eigenvalue $\hat{\lambda}(m,n)$ is the number

$$\#\left\{(i,j) \in \mathbb{Z}^2 \mid i^2 + ij + j^2 = m^2 + mn + n^2\right\}.$$

As usual the counting function $N_{\mathbb{T}}(\lambda)$ of the torus $\mathbb{T}$ is defined by

$$\begin{aligned} N_{\mathbb{T}}(\lambda) &= \#\left\{n \geq 1 \mid \lambda_n(\mathbb{T}) < \lambda\right\}, \\ &= \#\left\{(m,n) \in \mathbb{Z}^2 \mid \tfrac{16\pi^2}{9}(m^2 + mn + n^2) < \lambda\right\}. \end{aligned} \tag{3.5}$$

Lemma 3.1 *The counting function of the equilateral torus satisfies*

$$N_{\mathbb{T}}(\lambda) \geq \frac{3\sqrt{3}}{2}\frac{\lambda}{4\pi} - \frac{9}{2\pi}\sqrt{\lambda} + 1\,. \tag{3.6}$$

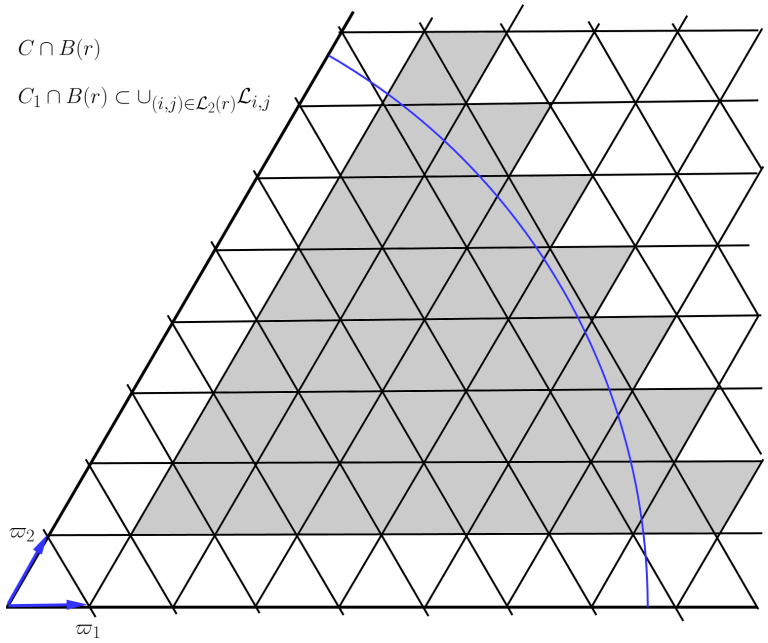

Figure 3.1: Illustration of (3.11)

Proof. The lemma follows from easy counting arguments. Define the sets[1]

$$\begin{aligned} C &= \{x\varpi_1 + y\varpi_2 \mid x, y > 0\}\,, \\ C_1 &= \{x\varpi_1 + y\varpi_2 \mid x, y > 1\}\,, \\ B(r) &= \{x \in \mathbb{E}^2 \mid |x| < r\}\,. \end{aligned} \tag{3.7}$$

For $(i, j) \in \mathbb{Z}^2$, define the closed lozenge $\mathcal{L}_{i,j}$,

$$\mathcal{L}_{i,j} = \{x\varpi_1 + y\varpi_2 \mid i \le x \le i + 1,\, j \le y \le j + 1\}\,. \tag{3.8}$$

Define the sets

$$\begin{aligned} \mathcal{L}(r) &= \{(i, j) \in \mathbb{Z}^2 \mid i\varpi_1 + j\varpi_2 \in B(r)\}\ , \\ \mathcal{L}_2(r) &= \{(i, j) \in \mathbb{Z}^2 \mid i\varpi_1 + j\varpi_2 \in C \cap B(r)\}\ , \\ \mathcal{L}_1(r) &= \{i \in \mathbb{Z} \mid i \ge 1 \text{ and } i\varpi_1 \in B(r)\}\ . \end{aligned} \tag{3.9}$$

Denote by $A(\Omega)$ the area of the set Ω contained in $\mathbb{E}^2$ or $\mathbb{T}$. Define h_ϖ to be the height of the equilateral triangle $(0, \varpi_1, \varpi_2)$, i.e., $h_\varpi = \frac{1}{\sqrt{3}}$, and define A_ϖ to be the area of the lozenges $\mathcal{L}_{i,j}$.

For symmetry reasons, we have the relation

$$\#\mathcal{L}(r) = 6\,\#\mathcal{L}_2(r) + 6\,\#\mathcal{L}_1(r) + 1\,. \tag{3.10}$$

Furthermore, see Figure 3.1, it is easy to check, that

$$C_1 \cap B(r) \subset \bigcup_{(i,j)\in\mathcal{L}_2(r)} \mathcal{L}_{i,j}. \tag{3.11}$$

[1]The set C is an open Weyl chamber [6].

It follows that $A_\varpi \#\mathcal{L}_2(r) \geq A(C_1 \cap B(r))$, and hence that

$$A_\varpi \#\mathcal{L}_2(r) \geq A(C \cap B(r)) - 2rh_\varpi + A_\varpi.$$

Using the fact that $h_\varpi = \frac{1}{\sqrt{3}}$ and $A_\varpi = \frac{2}{3\sqrt{3}}$, we obtain that

$$\#\mathcal{L}_2(r) \geq \frac{\sqrt{3}\pi}{4} r^2 - 3r + 1\,. \tag{3.12}$$

Similarly, since $|\varpi_1| = \frac{2}{3}$, we have that

$$\#\mathcal{L}_1(r) = \left[\frac{r}{|\varpi_1|}\right] \geq \frac{3}{2} r - 1\,. \tag{3.13}$$

Finally, we obtain

$$\#\mathcal{L}(r) \geq \frac{3\sqrt{3}\pi}{2} r^2 - 9r + 1\,. \tag{3.14}$$

Since $N_{\mathbb{T}}(\lambda) = \#\mathcal{L}(\frac{\sqrt{\lambda}}{2\pi})$, we obtain the estimate

$$N_{\mathbb{T}}(\lambda) \geq \frac{3\sqrt{3}}{2} \frac{\lambda}{4\pi} - \frac{9}{2\pi}\sqrt{\lambda} + 1\,. \tag{3.15}$$

□

Remark. Notice that the area of the equilateral torus is

$$A(\mathbb{T}) = \frac{3\sqrt{3}}{2}\,,$$

so that the above lower bound is asymptotically sharp (Weyl's asymptotic law).

Denote by $a(\mathbb{T})$ the length of the shortest closed geodesic on the flat torus $\mathbb{T}$ i.e.,

$$a(\mathbb{T}) = \frac{\sqrt{3}}{2} |\alpha_1^\vee| = \frac{3}{2}\,. \tag{3.16}$$

According to [11, §7], we get in the particular case of the torus the following isoperimetric inequality

Lemma 3.2 *If a domain $\Omega \subset \mathbb{T}$ has area $A(\Omega) \leq \frac{(a(\mathbb{T}))^2}{\pi}$, then the length $\ell(\partial\Omega)$ of its boundary satisfies*

$$\ell^2(\partial\Omega) \geq 4\pi A(\Omega)\,.$$

Together with (3.16), this implies the

Proposition 3.3 *Let $\Omega \subset \mathbb{T}$ be a domain whose area satisfies $A(\Omega) \leq \frac{9}{4\pi}$. Then, the first Dirichlet eigenvalue of Ω satisfies the inequality*

$$\lambda(\Omega) \geq \frac{\pi j_{0,1}^2}{A(\Omega)}\,, \tag{3.17}$$

where $j_{0,1}$ is the first positive zero of the Bessel function of order 0.

We recall that $j_{0,1} \sim 2.4048255577$.

Proof. Apply the proof of the classical Faber-Krahn inequality given for example in [8]. □

3.2 Courant-sharp eigenvalues of the equilateral torus

If $\lambda_n = \lambda_n(\mathbb{T})$ is Courant-sharp, then $\lambda_{n-1}(\mathbb{T}) < \lambda_n(\mathbb{T})$ and hence $N_{\mathbb{T}}(\lambda_n) = n-1$. In view of Lemma 3.1, we obtain

$$\frac{3\sqrt{3}}{8\pi}\lambda_n - \frac{9}{2\pi}\sqrt{\lambda_n} - (n-2) \leq 0\,.$$

It follows that

$$\lambda_n(\mathbb{T}) \text{ Courant-sharp } \Rightarrow \lambda_n(\mathbb{T}) \leq 12\left(1+\sqrt{1+\frac{2\pi}{9\sqrt{3}}(n-2)}\right)^2\,. \tag{3.18}$$

If λ_n is Courant-sharp, there exists an eigenfunction u associated with λ_n with exactly n nodal domains. One of them, call it Ω, satisfies

$$A(\Omega) \leq \frac{A(\mathbb{T})}{n} = \frac{3\sqrt{3}}{2n}\,.$$

If $n \geq 4$, Ω satisfies the assumption of Proposition 3.3 and hence,

$$\lambda_n(\mathbb{T}) = \lambda(\Omega) \geq \frac{\pi j_{0,1}^2}{A(\Omega)}\,.$$

It follows that

$$n \geq 4 \text{ and } \lambda_n(\mathbb{T}) \text{ Courant-sharp } \Rightarrow \lambda_n(\mathbb{T}) \geq \frac{2\pi j_{0,1}^2}{3\sqrt{3}}\,n\,. \tag{3.19}$$

Comparing (3.18) and (3.19), we see that if the eigenvalue is Courant-sharp, then $n \leq 63$. **Hence it remains to examine condition** (3.19) **for the first** 63 **eigenvalues.**

The following table gives the first 85 normalized eigenvalues $\bar{\lambda}_k$ such that

$$\lambda_k = \frac{16\pi^2}{9}\bar{\lambda}_k\,.$$

The condition (3.19) becomes

$$n \geq 4 \text{ and } \lambda_n(\mathbb{T}) \text{ Courant-sharp } \Rightarrow \frac{\bar{\lambda}_n(\mathbb{T})}{n} \geq \frac{\sqrt{3}j_{0,1}^2}{8\pi} \sim 0.3985546913\,. \tag{3.20}$$

The first column in the table displays the normalized eigenvalue $\bar{\lambda}$; the second column the least integer k such that $\bar{\lambda}_k = \bar{\lambda}$; the third column the largest integer k sur that $\bar{\lambda}_k = \bar{\lambda}$; the fourth column the multiplicity of $\bar{\lambda}$. The last column displays the ratio $\bar{\lambda}_k/k$ which should be larger than 0.3985546913 provided that $n \geq 4$ and λ_n is Courant-sharp.

eigenvalue	minimum index	maximum index	multiplicity	ratio
0	1	1	1	
1	2	7	6	
3	8	13	6	0.3750000000
4	14	19	6	0.2857142857
7	20	31	12	0.3500000000
9	32	37	6	0.2812500000
12	38	43	6	0.3157894737
13	44	55	12	0.2954545455
16	56	61	6	0.2857142857
19	62	73	12	0.3064516129
21	74	85	12	0.2837837838

Remark. The ratio $\bar{\lambda}_n(\mathbb{T})/n$ is meaningful to study Courant-sharpness for $n \geq 4$ only. This is why this information is not calculated in the first two lines.

4 The equilateral triangle: spectrum and action of symmetries

In this section, we start the analysis of the case of the equilateral triangle by recalling its spectrum and exploring the action of symmetries in each eigenspace of multiplicity 2. We keep the notation of the previous sections.

4.1 Eigenvalues and eigenfunctions

Recall the following result [2, Proposition 9].

Proposition 4.1 *Up to normalization, a complete set of eigenfunctions of the Dirichlet Laplacian in the equilateral triangle $\mathcal{T} = \{0, A, B\}$, with sides of length 1, is given by the functions*

$$\begin{array}{rcl} \Phi_p & = & \sum_{w\in W} \epsilon(w)\phi_{w(p)}\,, \\ \Phi_p(x) & = & \sum_{w\in W} \epsilon(w) \exp\left(2i\pi\langle x, w(p)\rangle\right)\,, \end{array} \tag{4.1}$$

where p ranges over the set $C\cap\Gamma^*$, and where $\epsilon(w)$ is the determinant of w. The associated eigenvalues are the numbers $4\pi^2|p|^2$ for $p \in C \cap \Gamma^*$. The multiplicity of the eigenvalue $4\pi^2|p|^2$ is given by $\#\{q \in C \cap \Gamma^* \mid |q| = |p|\}$.

Remark. Notice that

$$C \cap \Gamma^* = \{m\varpi_1 + n\varpi_2 \mid m, n \in \mathbb{N}^\bullet\}\,,$$

so that the eigenvalues of the equilateral triangle $\mathcal{T}$, with sides of length 1, are the numbers

$$\frac{16\pi^2}{9}(m^2 + mn + n^2) \text{ for } m, n \in \mathbb{N}^\bullet\,.$$

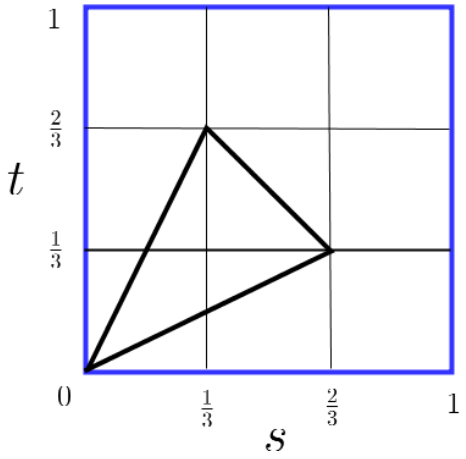

Figure 4.1: Parametrization $\mathcal{F}$

Idea of the proof.
We follow [2]. Given a Dirichlet eigenfunction ϕ of the triangle, we extend it to a function ψ on $\mathbb{E}^2$ using the symmetries $s_{i,k}$, in such a way that $\psi \circ w = \epsilon(w)\psi$ for any w in the group W_a. This is possible because $\mathcal{T}$ is a fundamental domain for W_a. The function ψ turns out to be smooth. Because $W_a = \Gamma \rtimes W$, the function ψ is Γ-periodic, and hence defines an eigenfunction Φ on the torus $\mathbb{E}^2/\Gamma$ which satisfies $\Phi \circ w = \epsilon(w)\Phi$ for all $w \in W$. Conversely, any eigenfunction Φ on the torus, which satisfies this condition, gives a Dirichlet eigenfunction of the triangle. It remains to identify the eigenfunctions of the torus which satisfy the condition. This is done by making use of [6, Proposition 1, §VI.3]. □

The Dirichlet eigenfunctions of $\mathcal{T}$ look a little simpler in the following parametrization $\mathcal{F}$ of $\mathbb{E}^2$,

$$\begin{aligned} \mathcal{F} &: \mathbb{R}^2 \to \mathbb{E}^2\,, \\ \mathcal{F} &: (s,t) \mapsto s\alpha_1^\vee + t\alpha_2^\vee\,. \end{aligned} \tag{4.2}$$

Given a point $p \in \mathbb{E}^2$, we will denote by (x, y) its coordinates with respect to the standard basis $\{e_1, e_2\}$, and by $(s, t)_\mathcal{F}$ its coordinates in the parametrization $\mathcal{F}$. More precisely, we will write,

$$\begin{cases} p = (x,y), & \text{for } p = xe_1 + ye_2, \\ p = (s,t)_\mathcal{F} & \text{for } p = s\alpha_1^\vee + t\alpha_2^\vee. \end{cases} \tag{4.3}$$

In the parametrization $\mathcal{F}$, a fundamental domain for the action of Γ on $\mathbb{R}^2$ is the square $\{0 \le s \le 1\} \times \{0 \le t \le 1\}$; a fundamental domain for the action of W_a on $\mathbb{R}^2$ is the triangle with vertices $(0,0)_\mathcal{F}$, $(\frac{2}{3}, \frac{1}{3})_\mathcal{F}$ and $(\frac{1}{3}, \frac{2}{3})_\mathcal{F}$, see Figure 4.1.

Notice that the parametrization $\mathcal{F}$ is not orthogonal, and that the Laplacian is given in this parametrization by

$$\Delta_\mathcal{F} = \frac{4}{9}\left(\partial_{ss}^2 + \partial_{st}^2 + \partial_{tt}^2\right)\,. \tag{4.4}$$

Recall that the function ϕ_p is defined by $\phi_p(x) = \exp\left(2i\pi\langle x, p\rangle\right)$, for $x \in \mathbb{E}^2$ and $p \in \Gamma$. In the parametrization $\mathcal{F}$, writing $x = s\alpha_1^\vee + t\alpha_2^\vee$ and $p = m\varpi_1 + n\varpi_2$, the function ϕ_p

will be written as

$$\phi_{m,n}(s,t) = \exp\left(2i\pi(ms+nt)\right). \tag{4.5}$$

To write the eigenfunctions of the Dirichlet Laplacian in the equilateral triangle, we have to compute the scalar products $\langle x, w(p)\rangle$ or equivalently $\langle w(x), p\rangle$ for $x = s\alpha_1^\vee + t\alpha_2^\vee$ and $p = m\varpi_1 + n\varpi_2$. Table 4.1 displays the result.

w	$\det(w)$	$\langle w(x), p\rangle$
1	1	$ms+nt$
s_1	-1	$-ms+(m+n)t$
s_2	-1	$(m+n)s-nt$
s_3	-1	$-ns-mt$
$s_1 \circ s_2$	1	$ns-(m+n)t$
$s_2 \circ s_1$	1	$-(m+n)s+mt$

Table 4.1: Action of W

Define the functions

$$\begin{aligned} E_{m,n}(s,t) = &\exp\big(2i\pi\big(ms+nt\big)\big) - \exp\big(2i\pi\big(-ms+(m+n)t\big)\big) \\ &- \exp\big(2i\pi\big((m+n)s-nt\big)\big) - \exp\big(2i\pi\big(-ns-mt\big)\big) \\ &+ \exp\big(2i\pi\big(ns-(m+n)t\big)\big) + \exp\big(2i\pi\big(-(m+n)s+mt\big)\big)\,, \end{aligned} \tag{4.6}$$

Using Table 4.1, we see that

$$E_{n,m}(s,t) = -\overline{E_{m,n}(s,t)}\,. \tag{4.7}$$

Looking at the pairs $[m,n]$ and $[n,m]$ simultaneously, and making use of real eigenfunctions instead of complex ones, we find that eigenfunctions associated with the pairs of positive integers $[m,n]$ and $[n,m]$, are $C_{m,n}(s,t)$ and $S_{m,n}(s,t)$, given by the following formulas,

$$\begin{aligned} C_{m,n}(s,t) = &\cos 2\pi\big(ms+nt\big) - \cos 2\pi\big(-ms+(m+n)t\big) \\ &- \cos 2\pi\big((m+n)s-nt\big) - \cos 2\pi\big(-ns-mt\big) \\ &+ \cos 2\pi\big(ns-(m+n)t\big) + \cos 2\pi\big(-(m+n)s+mt\big)\,, \end{aligned} \tag{4.8}$$

and

$$\begin{aligned} S_{m,n}(s,t) = &\sin 2\pi\big(ms+nt\big) - \sin 2\pi\big(-ms+(m+n)t\big) \\ &- \sin 2\pi\big((m+n)s-nt\big) - \sin 2\pi\big(-ns-mt\big) \\ &+ \sin 2\pi\big(ns-(m+n)t\big) + \sin 2\pi\big(-(m+n)s+mt\big)\,. \end{aligned} \tag{4.9}$$

Remarks. Notice that by (4.7) $C_{m,n} = -C_{n,m}$ and $S_{m,n} = S_{n,m}$. The line $\{s=t\}$ corresponds to the median of the equilateral triangle $\mathcal{T}$ issued from O. This median divides

$\mathcal{T}$ into two congruent triangles with angles $\{30, 60, 90\}$ degrees. The eigenfunctions $C_{m,n}$ correspond to the Dirichlet eigenfunctions of these triangles. When $m = n$, we have $C_{m,m} \equiv 0$ and

$$S_{m,m}(s,t) = 2\left\{\sin 2\pi m(s+t) \ - \sin 2\pi m(2t-s) - \sin 2\pi m(2s-t)\right\} \ ,$$

i.e.,

$$S_{m,m}(s,t) = S_{1,1}(ms, mt)\,. \tag{4.10}$$

4.2 Symmetries

Call F_C the centroid of the equilateral triangle $\mathcal{T} = \{0, A, B\}$. With the conventions (4.3), $F_C = (\frac{1}{2}, \frac{\sqrt{3}}{6}) = (\frac{1}{3}, \frac{1}{3})_{\mathcal{F}}$. The isometry group $G_{\mathcal{T}}$ of the triangle $\mathcal{T}$ has six elements: the three orthogonal symmetries with respect to the medians of the triangle (which fix one vertex and exchange the two other vertices), the rotations $\rho_{\pm}$, with center F_C and angles $\pm\frac{2\pi}{3}$ (which permute the vertices), and the identity. The group $G_{\mathcal{T}}$ fixes the centroid F_C.

In the parametrization $\mathcal{F}$, the symmetries are given by

$$\begin{aligned} \sigma_1(s,t) &= (t,s)\,, \\ \sigma_2(s,t) &= (-s+\tfrac{2}{3}, t-s+\tfrac{1}{3})\,, \\ \sigma_3(s,t) &= (s-t+\tfrac{1}{3}, -t+\tfrac{2}{3})\,. \end{aligned} \tag{4.11}$$

i.e., respectively, the symmetries with respect to the median issued from 0, to the median issued from B, and to the median issued from A.

As a matter of fact, the group $G_{\mathcal{T}}$ is generated by the symmetries σ_1 and σ_2. The rotations are

$$\rho_+ = \sigma_2 \circ \sigma_1 : (s,t) \mapsto (-t + \frac{2}{3}, s - t + \frac{1}{3}),$$

with angle $\frac{2\pi}{3}$, and

$$\rho_- = \sigma_1 \circ \sigma_2 : (s,t) \mapsto (t - s + \frac{1}{3}, -s + \frac{2}{3}),$$

with angle $-\frac{2\pi}{3}$. Furthermore, $\sigma_3 = \sigma_1 \circ \sigma_2 \circ \sigma_1 = \sigma_2 \circ \sigma_1 \circ \sigma_2$.

The action of the symmetries σ_1, σ_2 on the eigenfunctions $C_{m,n}$ and $S_{m,n}$ is given by

$$\begin{aligned} \sigma_1^* C_{m,n} &= -C_{m,n}\,, \\ \sigma_1^* S_{m,n} &= S_{m,n}\,, \\ \sigma_2^* C_{m,n} &= -\cos\alpha_{m,n}\, C_{m,n} - \sin\alpha_{m,n}\, S_{m,n}\,, \\ \sigma_2^* C_{m,n} &= -\sin\alpha_{m,n}\, C_{m,n} + \cos\alpha_{m,n}\, S_{m,n}\,, \end{aligned} \tag{4.12}$$

where $\alpha_{m,n} = \frac{2\pi(2m+n)}{3}$.

Working in the parametrization $\mathcal{F}$ and using the convention (4.3), we define for the analysis of the zero set of any eigenfunction associated with $\frac{16\pi^2}{9}(m^2+mn+n^2)$ (in the case of multiplicity 2) the family

$$\Psi^{\theta}_{m,n}(s,t) = \cos\theta\, C_{m,n}(s,t) + \sin\theta\, S_{m,n}(s,t)\,. \tag{4.13}$$

The action of the symmetries on the family $\Psi^{\theta}_{m,n}$ defined by (4.13) is given by

$$\begin{aligned} \sigma_1^*\Psi^{\theta}_{m,n} &= \Psi^{\pi-\theta}_{m,n}\,, \\ \sigma_2^*\Psi^{\theta}_{m,n} &= \Psi^{\pi+\alpha_{m,n}-\theta}_{m,n}\,, \\ \sigma_3^*\Psi^{\theta}_{m,n} &= \Psi^{\pi-\alpha_{m,n}-\theta}_{m,n}\,. \end{aligned} \tag{4.14}$$

5 Pleijel's approach for Courant-sharp eigenvalues

In order to investigate the Courant-sharp Dirichlet eigenvalues of the equilateral triangle $\mathcal{T}$, we use the same methods as in [18] and Section 3.

Notice that the counting function of the Dirichlet eigenvalues of the equilateral triangle is given by

$$N_{\mathcal{T}}(\lambda) = \mathcal{L}_2(\frac{\sqrt{\lambda}}{2\pi}) = \#\left\{(k,\ell)\in\mathbb{N}^\bullet\times\mathbb{N}^\bullet \mid |k\varpi_1+\ell\varpi_2|^2 < \frac{\lambda}{4\pi^2}\right\}. \tag{5.1}$$

Using (3.12), we conclude that

$$N_{\mathcal{T}}(\lambda) \geq \frac{\sqrt{3}}{4}\frac{\lambda}{4\pi} - \frac{3}{2\pi}\sqrt{\lambda} + 1\,. \tag{5.2}$$

Notice that this lower bound is asymptotically sharp (Weyl's asymptotic law).

Assuming that $\lambda_n(\mathcal{T})$ is Courant-sharp, we have $\lambda_{n-1}(\mathcal{T}) < \lambda_n(\mathcal{T})$, and hence $N_{\mathcal{T}}(\lambda_n(\mathcal{T})) = n-1$. It follows that

$$\lambda_n(\mathcal{T}) \text{ Courant-sharp } \Rightarrow \lambda_n(\mathcal{T}) \leq 48\left(1+\sqrt{1+\frac{\pi}{3\sqrt{3}}(n-2)}\right)^2. \tag{5.3}$$

On the other-hand, if $\lambda_n(\mathcal{T})$ is Courant-sharp, there exists an eigenfunction u with exactly n nodal domains $\Omega_1,\dots\Omega_n$, for which we can write

$$\lambda_n(\mathcal{T}) = \lambda(\Omega_i) \geq \frac{\pi j_{0,1}^2}{A(\Omega_i)}\,,$$

where we have used the Faber-Krahn inequality in $\mathbb{E}^2$.
Summing up in i, it follows that

$$\lambda_n(\mathcal{T}) \text{ Courant-sharp } \Rightarrow \frac{\lambda_n(\mathcal{T})}{n} \geq \frac{\pi j_{0,1}^2}{A(\mathcal{T})} = \frac{4\pi j_{0,1}^2}{\sqrt{3}}\,. \tag{5.4}$$

Combining (5.3) and (5.4), we find that if $\lambda_n(\mathcal{T})$ is Courant-sharp, then $n \leq 40$. It follows that to determine the Courant-sharp eigenvalues, it suffices to look at the first 40 eigenvalues of the equilateral triangle. Using (5.4) again, we compute the ratios $\frac{\bar{\lambda}_n(\mathcal{T})}{n}$ for the first 40 normalized eigenvalues ($\bar{\lambda}_n(\mathcal{T}) = \frac{9}{16\pi^2}\lambda_n(\mathcal{T})$), and compare them with the value

$$\frac{3\sqrt{3}j_{0,1}^2}{4\pi} \sim 2.391328148\,.$$

This is given by the following table in which the first column gives the normalized eigenvalue $\bar{\lambda}$; the second column the smallest index i such that $\bar{\lambda}_i = \bar{\lambda}$; the third column the largest index j such that $\bar{\lambda}_j = \bar{\lambda}$; the fourth column the multiplicity of $\bar{\lambda}$; and the last one the ratio normalized eigenvalue/least index (which is the relevant information for checking the Courant-sharp property).

$\bar{\lambda}$	$\bar{\lambda}_i = \bar{\lambda}$	$\bar{\lambda}_j = \bar{\lambda}$	mult($\bar{\lambda}$)	$\frac{\bar{\lambda}_i(\mathcal{T})}{i}$
3	1	1	1	**3**
7	2	3	2	**3.5**
12	4	4	1	**3**
13	5	6	2	**2.6000000**
19	7	8	2	**2.7142857**
21	9	10	2	2.333333333
27	11	11	1	**2.45454545**
28	12	13	2	2.333333333
31	14	15	2	2.214285714
37	16	17	2	2.312500000
39	18	19	2	2.166666667
43	20	21	2	2.150000000
48	22	22	1	2.181818182
49	23	24	2	2.130434783
52	25	26	2	2.080000000
57	27	28	2	2.111111111
61	29	30	2	2.103448276
63	31	32	2	2.032258065
67	33	34	2	2.030303030
73	35	36	2	2.085714286
75	37	37	1	2.027027027
76	38	39	2	2.
79	40	41	2	1.975000000

Table 5.1: Courant-sharp eigenvalues satisfy $\frac{\bar{\lambda}_n(\mathcal{T})}{n} \geq 2.391328148$

Lemma 5.1 *The only possible Courant-sharp eigenvalues of the equilateral triangle are the $\lambda_k(\mathcal{T})$, for $k \in \{1, 2, 4, 5, 7, 11\}$.*

Clearly, the eigenvalues λ_1 and λ_2 are Courant-sharp. The eigenvalues $\lambda_4 = \hat{\lambda}(2,2)$ and $\lambda_{11} = \hat{\lambda}(3,3)$ are simple. It is easy to see that the number of nodal domains is 4, *resp.* 9, for these eigenvalues, see (4.10) and Figure 5.1. Hence λ_4 is Courant sharp, and λ_{11} is not Courant sharp.

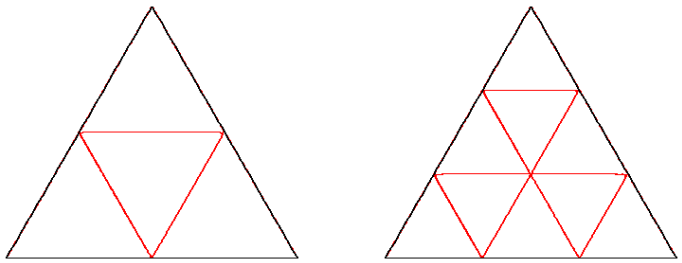

Figure 5.1: Nodal sets corresponding to λ_4 and λ_{11}

In order to determine the Courant-sharp eigenvalues, it therefore remains to consider the eigenvalues $\lambda_5 = \hat{\lambda}(1,3) = \hat{\lambda}(3,1)$ and $\lambda_7 = \hat{\lambda}(2,3) = \hat{\lambda}(3,2)$ which have multiplicity 2. We study these eigenvalues in Sections 7 and 8 respectively, see Figures 5.2 and 5.3.

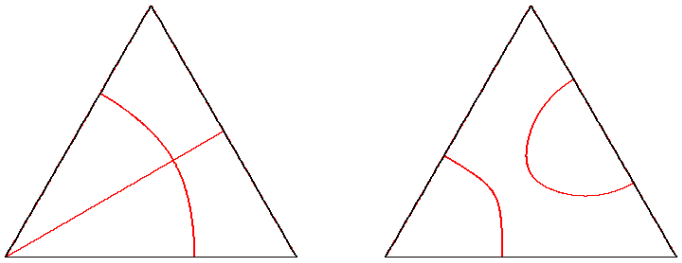

Figure 5.2: Nodal sets for the eigenfunctions $C_{1,3}$ and $S_{1,3}$ corresponding to λ_5

We will work in the triangle $\mathcal{T}$, with vertices $\{O, A, B\}$. We denote by F_C the centroid of the triangle. The median issued from the vertex O is denoted by $[OM]$, the mid-point of the side BA by M_O. We use similar notation for the other vertices, see Figure 5.4.

Remark. We denote by $N(\Psi^\theta_{m,n})$ the nodal set of the eigenfunction $\Psi^\theta_{m,n}$ i.e., the closure of the set of zeros of the eigenfunction in the interior of the triangle. The eigenfunctions also vanish on the edges of the triangles, and we will analyze separately the points in the open edges and the vertices. For a summary of the general properties of nodal sets of eigenfunctions, we refer to [5, Section 5]. Observe that the eigenfunctions $\Psi^\theta_{m,n}$ are defined over the whole plane, so that even at the boundary of the triangle, we can use the local structure of the nodal set.

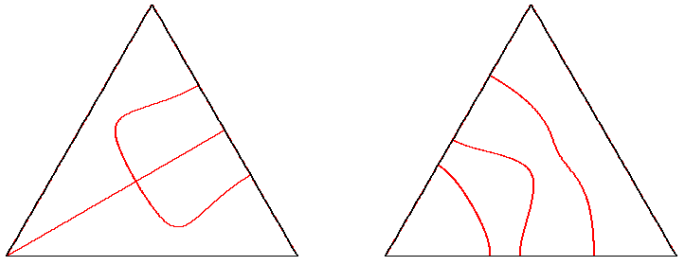

Figure 5.3: Nodal sets for the eigenfunctions $C_{2,3}$ and $S_{2,3}$ corresponding to λ_7

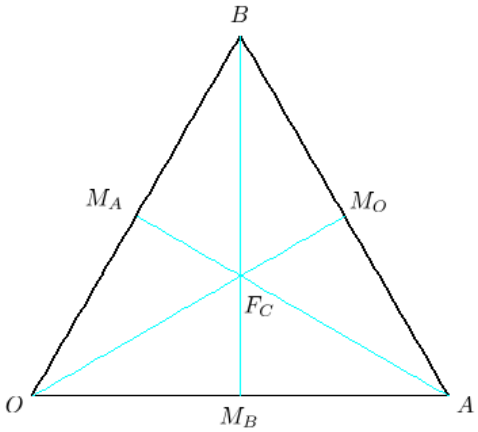

Point	$\mathbb{E}^2$	$\mathcal{F}$
Vertex O	$(0,0)$	$(0,0)_{\mathcal{F}}$
Vertex A	$(1,0)$	$(\frac{2}{3},\frac{1}{3})_{\mathcal{F}}$
Vertex B	$(\frac{1}{2},\frac{\sqrt{3}}{2})$	$(\frac{1}{3},\frac{2}{3})_{\mathcal{F}}$
Centroid F_C	$(\frac{1}{2},\frac{\sqrt{3}}{6})$	$(\frac{1}{3},\frac{1}{3})_{\mathcal{F}}$
Mid-point M_O	$(\frac{3}{2},\frac{\sqrt{3}}{4})$	$(\frac{1}{2},\frac{1}{2})_{\mathcal{F}}$
Mid-point M_A	$(\frac{1}{2},\frac{\sqrt{3}}{4})$	$(\frac{1}{6},\frac{1}{3})_{\mathcal{F}}$
Mid-point M_B	$(\frac{1}{2},0)$	$(\frac{1}{3},\frac{1}{6})_{\mathcal{F}}$

Figure 5.4: Triangle $\mathcal{T}$

The remaining part of this paper is devoted to the proof of Theorem 1.2, using the following strategy.

6 Playing on the checkerboard

After the reduction à la Pleijel, we now have to analyze the nodal picture of any eigenfunction in two 2-dimensional eigenspaces of the Laplacian in $\mathcal{T}$, the interior of the equilateral triangle. The nodal set $N(\Psi)$ of a Dirichlet eigenfunction Ψ is the closure of the set $\{x \in \mathcal{T} \mid \Psi(x) = 0\}$ in $\overline{\mathcal{T}}$. The function Ψ actually extends smoothly to the whole plane, and the nodal set of Ψ consists of finitely many regular arcs which may intersect, or hit the boundary of $\mathcal{T}$, with the equiangular property, [10, Section 2.1].

Let λ be either λ_5 or λ_7, and let $\mathcal{E}$ be the associated (2-dimensional) eigenspace. Determining whether λ is Courant-sharp amounts to describing the possible nodal sets of the family $\Psi^\theta = \cos\theta\, C + \sin\theta\, S$, where $\{C, S\}$ is a basis of $\mathcal{E}$, and $\theta \in [0, 2\pi]$. For this purpose, we use the following ideas.

1. Using the natural *symmetries* of the triangle, we restrict the analysis to $\theta \in [0, \frac{\pi}{6}]$.

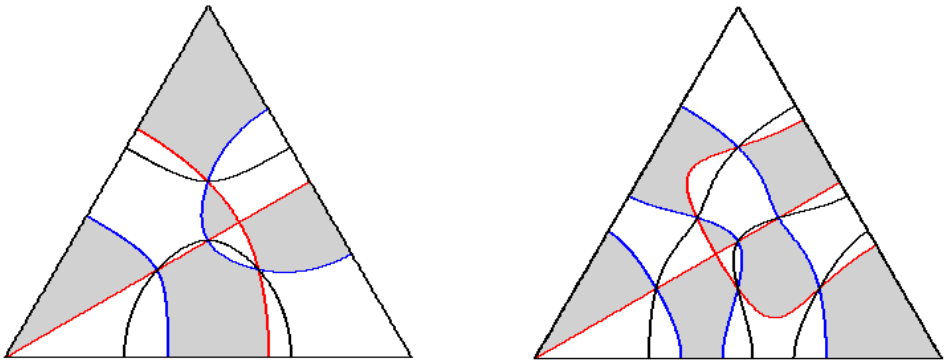

Figure 6.1: Checkerboards for λ_5 and λ_7, and nodal set $N(\Psi^{\frac{\pi}{6}})$

2. The set of *fixed points* $N(C) \cap N(S)$ i.e., the set of common zeros of the functions Ψ^θ, plays an important role in the analysis of the family of nodal sets $N(\Psi)$. When the variables are separated, as in the case of the square membrane, it is easy to determine the fixed points, [19, 5]. In the case of the equilateral triangle, we shall only determine the fixed points located on the medians of $\mathcal{T}$.

3. For $\theta \in]0, \frac{\pi}{6}]$, the nodal set $N(\Psi^\theta)$ is contained in the set $\{C\,S < 0\} \cup (N(C) \cap N(S))$, [19, 5]. This *checkerboard argument* is illustrated in Figure 6.1 which displays the checkerboards for λ_5 and λ_7, with $C = \Psi^0$ and $S = \Psi^{\frac{\pi}{2}}$, as well as the nodal set of $\Psi^{\frac{\pi}{6}}$ (Maple simulations). For the equilateral triangle, the variables are not separated, and we shall not use this argument directly, but rather *separation lemmas* involving the medians and other natural lines.

4. Critical zeros i.e., points at which both the eigenfunction and its first derivatives vanish, play a central role in our analysis. They are easy to determine when the variables are separated, [5]. In the case of the equilateral triangle, the determination of critical zeros is more involved. We first analytically determine the critical zeros on the boundary i.e., the points at which the nodal sets hits $\partial\mathcal{T}$. Later on in the proof, we show that Ψ^θ does not have interior critical zeros when $\theta \in]0, \frac{\pi}{6}]$. For this purpose, we use the following *energy argument*.

5. *Energy argument.* The medians divide the triangle $\mathcal{T}$ into six isometric semi-equilateral triangles, whose first Dirichlet eigenvalue is easily seen to be strictly larger than λ_7. This argument is needed to discard possible interior critical zeros, and also simply closed nodal arcs.

For a given $\theta \in]0, \frac{\pi}{6}]$, the above information provide some points in $N(\Psi^\theta)$. It remains to determine how the nodal arcs can join these points, without crossing the established barriers.

7 The eigenvalue $\lambda_5(\mathcal{T})$ and its eigenspace

We call $\mathcal{E}_5$ the 2-dimensional eigenspace associated with the eigenvalue $\lambda_5(\mathcal{T})$, i.e., with the pairs $[1,3]$ and $[3,1]$. Recall the eigenfunctions,

$$\begin{aligned} C_{1,3}(s,t) = \;& \cos 2\pi(s+3t) - \cos 2\pi(-s+4t) - \cos 2\pi(4s-3t) \\ & - \cos 2\pi(-3s-t) + \cos 2\pi(3s-4t) + \cos 2\pi(-4s+t)\,, \\ S_{1,3}(s,t) = \;& \sin 2\pi(s+3t) - \sin 2\pi(-s+4t) - \sin 2\pi(4s-3t) \\ & - \sin 2\pi(-3s-t) + \sin 2\pi(3s-4t) + \sin 2\pi(-4s+t)\,. \end{aligned} \tag{7.1}$$

In this section, we now study the family $\Psi^\theta_{1,3}$ more carefully.

7.1 Symmetries

Taking Subsection 4.2 into account, we find that

$$\begin{aligned} \sigma_1^*\Psi^\theta_{1,3} &= \Psi^{\pi-\theta}_{1,3}\,, \\ \sigma_2^*\Psi^\theta_{1,3} &= \Psi^{\frac{\pi}{3}-\theta}_{1,3}\,, \\ \sigma_3^*\Psi^\theta_{1,3} &= \Psi^{\frac{5\pi}{3}-\theta}_{1,3}\,, \\ (\sigma_2\circ\sigma_1)^*\Psi^\theta_{1,3} &= \Psi^{\frac{2\pi}{3}+\theta}_{1,3}\,, \\ (\sigma_1\circ\sigma_2)^*\Psi^\theta_{1,3} &= \Psi^{\frac{4\pi}{3}+\theta}_{1,3}\,. \end{aligned} \tag{7.2}$$

It follows that, up to multiplication by a scalar, and for $V \in \{O, A, B\}$, the eigenspace $\mathcal{E}_5$ contains a unique eigenfunction S_V, *resp.* a unique eigenfunction C_V, which is invariant, *resp.* anti-invariant, under the symmetry $\sigma_{i(V)}$ with respect to the median $[VM]$ issued from the vertex V, where $i(O) = 1, i(A) = 3$, and $i(B) = 2$. More precisely, we have

$$\begin{aligned} &S_O = \Psi^{\frac{\pi}{2}}_{1,3} \text{ and } C_O = \Psi^0_{1,3}\,, \\ &S_A = \Psi^{\frac{11\pi}{6}}_{1,3} \text{ and } C_A = \Psi^{\frac{4\pi}{3}}_{1,3}\,, \\ &S_B = \Psi^{\frac{7\pi}{6}}_{1,3} \text{ and } C_B = \Psi^{\frac{2\pi}{3}}_{1,3}\,. \end{aligned} \tag{7.3}$$

Note that C_O, *resp.* S_O, are the functions $C_{1,3}$, *resp.* $S_{1,3}$, and that,

$$\begin{aligned} &S_A = (\sigma_1\circ\sigma_2)^* S_O \text{ and } C_A = (\sigma_1\circ\sigma_2)^* C_O\,, \\ &S_B = (\sigma_2\circ\sigma_1)^* S_O \text{ and } C_B = (\sigma_2\circ\sigma_1)^* C_O\,. \end{aligned} \tag{7.4}$$

The eigenfunctions S_V, *resp.* C_V, are permuted under the action of the rotations $\rho_+ = \sigma_2\circ\sigma_1$ and $\rho_- = \sigma_1\circ\sigma_2$. The eigenspace $\mathcal{E}_5$ does not contain any non trivial rotation invariant eigenfunction.

Since $\Psi^{\theta+\pi}_{1,3} = -\Psi^\theta_{1,3}$, it follows from (7.2) that, up to the symmetries σ_i, the nodal sets of the family $\Psi^\theta_{1,3}$, $\theta \in [0, 2\pi]$ are determined by the nodal sets of the sub-family $\theta \in [0, \frac{\pi}{6}]$.

From now on, we assume that $\theta \in [0, \frac{\pi}{6}]$.

7.2 Behaviour at the vertices

The vertices of the equilateral triangle $\mathcal{T}$ belong to the nodal set $N(\Psi^\theta_{1,3})$ for all θ. For geometric reasons, the order of vanishing at a vertex is at least 3. More precisely,

Properties 7.1 *Behaviour of $\Psi^\theta_{1,3}$ at the vertices.*

1. *The function $\Psi^\theta_{1,3}$ vanishes at order 6 at O if and only if $\theta \equiv 0 \pmod{\pi}$; otherwise it vanishes at order 3.*
2. *The function $\Psi^\theta_{1,3}$ vanishes at order 6 at A if and only if $\theta \equiv \frac{\pi}{3} \pmod{\pi}$; otherwise it vanishes at order 3.*
3. *The function $\Psi^\theta_{1,3}$ vanishes at order 6 at B if and only if $\theta \equiv \frac{2\pi}{3} \pmod{\pi}$; otherwise it vanishes at order 3.*

In other words, up to multiplication by a scalar, the only eigenfunction $\Psi^\theta_{1,3}$ which vanishes at higher order at a vertex $V \in \{O, A, B\}$ is C_V, the anti-invariant eigenfunction with respect to the median issued from the vertex V. In particular, when $\theta \in]0, \frac{\pi}{6}]$, the three vertices are critical zeros of order three for the eigenfunction $\Psi^\theta_{1,3}$, and no interior nodal curve of such an eigenfunction can arrive at a vertex.

Proof. Compute the Taylor expansions of $\Psi^\theta_{1,3}$ at the points under consideration. □

7.3 Fixed points on the medians

Since the median $[OM]$ is contained in the nodal set $N(C_{1,3})$, the intersection points of $[OM]$ with $N(S_{1,3})$ are fixed points of the family $N(\Phi^\theta_{1,3})$, i.e., common zeros of the functions $\Psi^\theta_{1,3}$. If we parametrize $[OM]$ by $u \mapsto (u, u)$ with $u \in [0, \frac{1}{2}]$, we find that

$$S_{1,3}\big|_{[OM]}(u) = 2\sin(8\pi u) - 2\sin(6\pi u) - 2\sin(2\pi u)\,. \tag{7.5}$$

It follows that

$$S_{1,3}\big|_{[OM]}(u) = -8\sin(\pi u)\,\sin(3\pi u)\,\sin(4\pi u)\,. \tag{7.6}$$

The last formula shows that there are two fixed points on the open median $[OM]$, the centroid of the triangle $F_C = (\frac{1}{3}, \frac{1}{3})_{\mathcal{F}}$, and the point $F_O = (\frac{1}{4}, \frac{1}{4})_{\mathcal{F}}$.

Taking into account the action of $G_{\mathcal{T}}$ on the space $\mathcal{E}_5$, see (7.2)-(7.4), we infer that the points $F_A = (\frac{5}{12}, \frac{1}{3})_{\mathcal{F}}$ and $F_B = (\frac{1}{3}, \frac{5}{12})_{\mathcal{F}}$ are also common zeros for the family $\Psi^\theta_{1,3}$. They are deduced from F_O by applying the rotations $\rho_\pm$, and situated on the two other medians.

Using Taylor expansions, it is easy to check that the fixed points F_* are not critical zeros of the functions $\Psi^\theta_{1,3}$. In the neighborhood of the fixed points F_*, the nodal set consists of a single regular arc.

Remarks.
(i) Note that we do not claim to have determined all the fixed points of the family

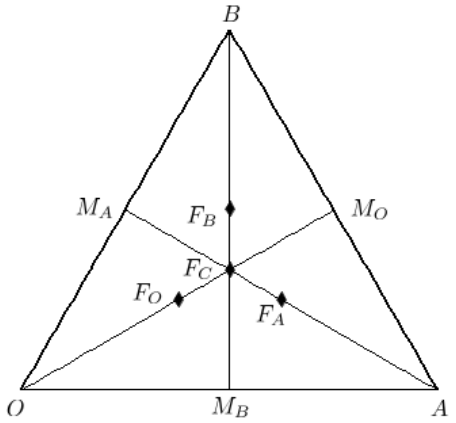

Point	$\mathbb{E}^2$	$\mathcal{F}$
Vertex O	$(0,0)$	$(0,0)_{\mathcal{F}}$
Vertex A	$(1,0)$	$(\frac{2}{3},\frac{1}{3})_{\mathcal{F}}$
Vertex B	$(\frac{1}{2},\frac{\sqrt{3}}{2})$	$(\frac{1}{3},\frac{2}{3})_{\mathcal{F}}$
Fixed point F_C	$(\frac{1}{2},\frac{\sqrt{3}}{6})$	$(\frac{1}{3},\frac{1}{3})_{\mathcal{F}}$
Fixed point F_O	$(\frac{3}{8},\frac{\sqrt{3}}{8})$	$(\frac{1}{4},\frac{1}{4})_{\mathcal{F}}$
Fixed point F_A	$(\frac{5}{8},\frac{\sqrt{3}}{8})$	$(\frac{5}{12},\frac{1}{3})_{\mathcal{F}}$
Fixed point F_B	$(\frac{1}{2},\frac{\sqrt{3}}{4})$	$(\frac{1}{3},\frac{5}{12})_{\mathcal{F}}$

Figure 7.1: Triangle $\mathcal{T}$ and fixed points for $\Psi^{\theta}_{1,3}$

$N(\Psi^{\theta}_{1,3})$ i.e., the set $N(C_{1,3}) \cap N(S_{1,3})$. We have so far only determined the fixed points located on the medians.
(ii) Notice that the fixed point F_O is the mid-point of the segment $[M_A M_B]$, *etc*.

7.4 Partial barriers for the nodal sets

We have seen that the family $\Psi^{\theta}_{1,3}$ has four fixed points, the centroid F_C of the triangle, and three other points F_O, F_A and F_B, located respectively on the open medians $[OM]$, $[AM]$, and $[BM]$, see Figure 7.1. As a matter of fact, the medians can serve as partial barriers.

Lemma 7.2 *For any θ, the nodal set $N(\Psi^{\theta}_{1,3})$ intersects each median at exactly two points unless the function $\Psi^{\theta}_{1,3}$ is one of the functions C_V for $V \in \{O, A, B\}$, in which case the corresponding median is contained in the nodal set. In particular, if $\theta \in]0, \frac{\pi}{6}]$, the nodal set $N(\Psi^{\theta}_{1,3})$ only meets the medians at the fixed points $\{F_O, F_A, F_B, F_C\}$.*

Proof. Use the following facts:
(i) the families $\{C_O, S_O\}$, $\{C_A, S_A\}$ and $\{C_B, S_B\}$ span $\mathcal{E}_5$;
(ii) the function C_V vanishes on the median issued from the vertex V. Write $\Psi^{\theta}_{1,3} = \alpha C_V + \beta S_V$. If $x \in [VM] \cap N(\Psi^{\theta}_{1,3})$, then $\beta S_V(x) = 0$. If $\beta \neq 0$, then $x \in \{F_C, F_V\}$. If $\beta = 0$, then $[VM] \subset N(\Psi^{\theta}_{1,3})$. □

Remark. A consequence of Lemma 7.2 and Subsection 7.3 is that for $\theta \in]0, \frac{\pi}{6}]$, no critical zero of the function $\Psi^{\theta}_{1,3}$ can occur on the medians.

The medians divide the equilateral triangle $\mathcal{T}$ into six isometric H-triangles (i.e., triangles with angles $\{30, 60, 90\}$ degrees), $T(F_C, O, M_B)$, *etc*. Each one of theses triangles is homothetic to the H-triangle $T(O, A, M_O)$ with scaling factor $\frac{1}{\sqrt{3}}$. On the other-hand, the first Dirichlet eigenvalue for the H-triangle $T(O, A, M_O)$ is $\lambda_2(\mathcal{T}) = 7$, with multiplicity 1, and associated eigenfunction $C_{1,3}$.

Lemma 7.3 *Let $\mathcal{T}_M$ denote the triangle $T(F_C, O, M_B)$. The first Dirichlet eigenvalue of the six H-triangles determined by the medians of $\mathcal{T}$ equals*

$$\lambda(\mathcal{T}_M) = 3\lambda_2(\mathcal{T}) = 21\,.$$

For $0 \le a \le 1$, define the line D_a by the equation $s + t = a$ in the parametrization $\mathcal{F}$.

$$D_a = \mathcal{F}\left(\{s + t = a\}\right)\,. \tag{7.7}$$

Lemma 7.4 *For $a \in \{\frac{1}{2}, \frac{2}{3}, \frac{3}{4}\}$, the intersections of the lines D_a with the nodal sets $N(C_{1,3})$ and $N(S_{1,3})$ are as follows.*

$$\begin{array}{lll} D_{\frac{1}{2}} \cap N(C_{1,3}) = \{F_O\}, & \textit{and} & D_{\frac{1}{2}} \cap N(S_{1,3}) = \{F_O\}, \\ D_{\frac{2}{3}} \cap N(C_{1,3}) = \{F_C, G_A, G_B\}, & \textit{and} & D_{\frac{2}{3}} \cap N(S_{1,3}) = \{F_C\}, \\ D_{\frac{3}{4}} \cap N(C_{1,3}) = \{F_A, F_B, G_O\}, & \textit{and} & D_{\frac{3}{4}} \cap N(S_{1,3}) = \{F_A, F_B\}, \end{array} \tag{7.8}$$

where G_A and G_B are symmetrical with respect to $[OM]$, and $G_O = (\frac{3}{8}, \frac{3}{8})_{\mathcal{F}}$. The lines are tangent to $N(S_{2,3})$ at the points F_O and F_C.

Proof. The segment $D_a \cap \mathcal{T}$ is parametrized by $u \mapsto (u, a - u)$ for $u \in [\frac{a}{3}, \frac{2a}{3}]$. For each value $a \in \{\frac{1}{2}, \frac{2}{3}, \frac{3}{4}\}$, define

$$\begin{array}{l} BC_a(u) = C_{2,3}(u, a - u), \quad u \in [\frac{a}{3}, \frac{2a}{3}]\,, \\ BS_a(u) = S_{2,3}(u, a - u), \quad u \in [\frac{a}{3}, \frac{2a}{3}]\,. \end{array} \tag{7.9}$$

Taking $a = \frac{1}{2}$, we find

$$\begin{array}{l} BC_{\frac{1}{2}}(u) = -4\sin(2\pi u)\sin(12\pi u)\,, \\ BS_{\frac{1}{2}}(u) = 4\cos(2\pi u)\sin(12\pi u)\,. \end{array} \tag{7.10}$$

Similarly,

$$\begin{array}{l} BC_{\frac{2}{3}}(u) = -2\sqrt{3}\sin(9\pi u)\cos(5\pi u + \frac{\pi}{3})\,, \\ BS_{\frac{2}{5}}(u) = -2\sqrt{3}\sin(9\pi u)\sin(5\pi u + \frac{\pi}{3})\,. \end{array} \tag{7.11}$$

$$\begin{array}{l} BC_{\frac{3}{4}}(u) = -2\sin(12\pi u)\left(\sin(2\pi u) + \cos(2\pi u)\right)\,, \\ BS_{\frac{3}{4}}(u) = -2\sin(12\pi u)\left(\sin(2\pi u) - \cos(2\pi u)\right)\,. \end{array} \tag{7.12}$$

Looking at the zeros of the above functions in the respective intervals, the lemma follows. □

The lemmas are illustrated by Figure 7.2 which displays the partial barriers (thin segments), and the nodal sets computed with Maple (thicker lines).

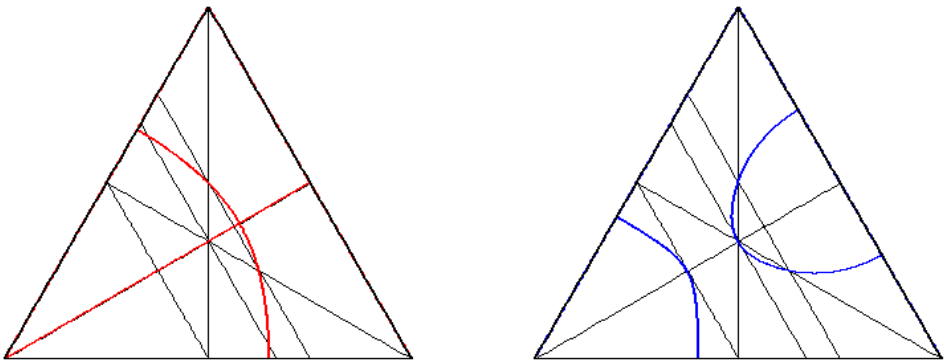

Figure 7.2: Partial barriers for $N(C_{1,3})$ and $N(S_{1,3})$

7.5 Critical zeros of $C_{1,3}$ and $S_{1,3}$ on the sides of $\mathcal{T}$, and on the median $[OM]$

Define the functions

$$\begin{array}{ll} FC(u) & := -\sin(7\pi u) + 3\sin(5\pi u) - 4\sin(2\pi u)\,, \\ FS(u) & := -\cos(7\pi u) - 3\cos(5\pi u) + 4\cos(2\pi u)\,, \end{array} \tag{7.13}$$

and the polynomials

$$\begin{array}{ll} P_C(x) & := 4x^2 + 4x - 1\,, \\ P_S(x) & := 4x^4 - x^2 + x - 1\,. \end{array} \tag{7.14}$$

Lemma 7.5 *The functions FC and FS satisfy,*

$$\begin{array}{ll} FC(u) & = -4\sin(\pi u)\left(\cos(\pi u) - 1\right)^2 \left(2\cos(\pi u) + 1\right)^2 \, P_C\left(\cos(\pi u)\right)\,, \\ FS(u) & = -4\left(\cos(\pi u) - 1\right)\left(2\cos(\pi u) + 1\right)^2 \, P_S\left(\cos(\pi u)\right)\,. \end{array} \tag{7.15}$$

Proof. Use the Chebyshev polynomials. □

Properties 7.6 *The partial derivatives of the functions $C_{1,3}$ and $S_{1,3}$ satisfy the following relations.*

1. *Parametrize the edge $[OA]$ by $u \mapsto (u, u/2)$, with $u \in [0, 2/3]$. Then,*

$$\begin{array}{ll} \partial_s C_{1,3}(u, u/2) = 2\pi FC(u)\,, & \partial_t C_{1,3}(u, u/2) = -4\pi FC(u)\,, \\ \partial_s S_{1,3}(u, u/2) = 2\pi FS(u)\,, & \partial_t S_{1,3}(u, u/2) = -4\pi FS(u)\,. \end{array} \tag{7.16}$$

2. *Parametrize the edge $[OB]$ by $u \mapsto (u/2, u)$, with $u \in [0, 2/3]$. Then,*

$$\begin{array}{ll} \partial_s C_{1,3}(u/2, u) = 4\pi FC(u)\,, & \partial_t C_{1,3}(u/2, u) = -2\pi FC(u)\,, \\ \partial_s S_{1,3}(u/2, u) = -4\pi FS(u)\,, & \partial_t S_{1,3}(u/2, u) = 2\pi FS(u)\,. \end{array} \tag{7.17}$$

3. *Parametrize the edge* $[BA]$ *by* $u \mapsto (u/2, 1-u/2)$, *with* $u \in [2/3, 4/3]$. *Then,*

$$\begin{array}{l} \partial_s C_{1,3}(u/2, 1-u/2) = -2\pi FC(u)\,, \quad \partial_t C_{1,3}(u/2, 1-u/2) = -2\pi FC(u)\,, \\ \partial_s S_{1,3}(u/2, 1-u/2) = 2\pi FS(u)\,, \quad \partial_t S_{1,3}(u/2, 1-u/2) = 2\pi FS(u)\,. \end{array} \tag{7.18}$$

Proof. It suffices to compute the partial derivatives of $C_{1,3}$ and $S_{1,3}$, and to make the substitutions corresponding to the parametrization of the edges. □

It follows from the above results that the critical zeros of $C_{1,3}$, *resp.* $S_{1,3}$, on $\partial\mathcal{T}$ are determined by the zeros of FC, *resp.* FS, in $[0, 4/3]$.

Lemma 7.7 *Zeros of* P_C *and* P_S.

1. *The polynomial* P_C *has only one root in the interval* $[-1, 1]$, *namely* $(\sqrt{2}-1)/2$.
2. *The polynomial* P_S *has exactly two roots in the interval* $[-1, 1]$, *namely* $\xi_- \approx -0.9094691258$ *and* $\xi_+ \approx 0.6638481772$.

Define the numbers

$$\begin{array}{rl} u_{1,C} &:= \frac{1}{\pi}\arccos(\frac{\sqrt{2}-1}{2}) \approx 0.433595245\,, \\ u_{1,S} &:= \frac{1}{\pi}\arccos(x_+) \approx 0.2689221041\,, \\ u_{2,S} &:= \frac{1}{\pi}\arccos(x_-) \approx 0.8635116189\,, \\ u_{3,S} &:= 2 - u_{2,S} \approx 1.136488381\,. \end{array} \tag{7.19}$$

The function FC vanishes at $0, \frac{2}{3}$, 1 and $\frac{4}{3}$, and has one simple zero $u_{1,C} \in]0, \frac{2}{3}[$. The function FS vanishes at $0, \frac{2}{3}$ and $\frac{4}{3}$. It has one simple zero $u_{1,S} \in]0, \frac{2}{3}[$, and two simple zeros $u_{2,S}, u_{3,S} \in]\frac{2}{3}, \frac{4}{3}[$.

Properties 7.8 *Critical zeros of the functions* $C_{1,3}$ *and* $S_{1,3}$ *on the open edges of* $\mathcal{T}$.

1. *The function* $C_{1,3}$ *has one critical zero* $Z_{1,C} = (u_{1,C}, u_{1,C}/2)_{\mathcal{F}}$ *on the open edge* $[OA]$; *one critical zero* $Z_{2,C} = (u_{1,C}/2, u_{1,C})_{\mathcal{F}}$ *on the open edge* $[OB]$; *one critical zero* $Z_{3,C} = M_O = (1/2, 1/2)_{\mathcal{F}}$ *on the open edge* $[BA]$. *These critical zeros have order* 2.
2. *The function* $S_{1,3}$ *has one critical zero* $Z_{1,S} = (u_{1,S}, u_{1,S}/2)_{\mathcal{F}}$ *on the open edge* $[OA]$; *one critical zero* $Z_{2,S} = (u_{1,S}/2, u_{1,S})_{\mathcal{F}}$ *on the open edge* $[OB]$; *two critical zeros* $Z_{3,S} = (u_{2,S}/2, 1-u_{2,S}/2)_{\mathcal{F}}$ *and* $Z_{4,S} = (u_{3,S}/2, 1-u_{3,S}/2)_{\mathcal{F}}$ *on the open edge* $[BA]$, *these points are symmetrical with respect to the point* M_O. *These critical zeros have order* 2.

Proof. Use Properties 7.6 and Lemma 7.7. □

Remark. The vertex O is a critical zero of order 6 of $C_{1,3}$, and a critical zero of order 3 of $S_{1,3}$. The vertices A and B are critical zeros of order 3 of both $C_{1,3}$ and $S_{1,3}$, see Properties 7.1.

Properties 7.9 *Critical zeros of the functions $C_{1,3}$ and $S_{1,3}$ on the median $[OM_O]$.*

1. *The function $C_{1,3}$ has one critical zero at O; one critical zero $Z_{5,C}$ of order 2 , where*

$$Z_{5,C} = (u_{5,C}/2, u_{5,C}/2)_{\mathcal{F}}, \text{ with } u_{5,C} := 1 - \arccos(3/4)/\pi \approx 0.7699465439\,;$$

   one critical zero $M_O = Z_{3,C}$ of order 2 .

2. *The function $S_{1,3}$ has no critical zero on the median $[OM]$, except the point O.*

Proof. Since $C_{1,3}$ vanishes on the median, its critical zeros on the median are the common zeros of its partial derivatives. They are precisely the zeros of the function

$$2\sin(4\pi u) - 5\sin(3\pi u) + 7\sin(\pi u)\,,$$

if we parametrize the median by $u \mapsto (u/2, u/2)$ for $u \in [0,1]$. The above function can be factorized as

$$4\sin(\pi u)\big(4\cos(\pi u) + 3\big)\big(\cos(\pi u) - 1\big)^2\,,$$

and the first assertion follows.

For the second assertion, we have to look for the common zeros of the function $S_{1,3}$ and its derivatives on the median. This amounts to finding the common zeros of the functions

$$2\sin(4\pi u) - 2\sin(3\pi u) - 2\sin(\pi u)\,,$$

and

$$4\cos(4\pi u) - 3\cos(3\pi u) - \cos(\pi u)\,.$$

The first function factorizes as

$$-8\sin(\frac{\pi u}{2})\sin(\frac{3\pi u}{2})\sin(2\pi u)\,.$$

It is easy to check that the only common zero is $u = 0$. □

Figure 7.3 displays the critical zeros of $C_{1,3}$ and $S_{1,3}$.

We state the following corollary of Proposition 7.9 for later reference.

Recall (see the notation (7.3)) that $\Psi_{1,3}^{\frac{\pi}{6}} = -S_B$, and that $S_B = \rho_+^* S_O$.

Corollary 7.10 *Critical zeros of the function S_B.*

1. *The function S_B has two critical zeros of order 2 on the side $[OA]$,*

$$Z_{3,S_B} = \rho_-(Z_{3,S}) \text{ and } Z_{4,S_B} = \rho_-(Z_{4,S})\,.$$

2. *The function S_B has one critical zero of order 2 on the side $[OB]$,*

$$Z_{1,S_B} = \rho_-(Z_{1,S})\,.$$

3. *The function S_B has one critical zero of order 2 on the side $[BA]$,*

$$Z_{2,S_B} = \rho_-(Z_{2,S})\,.$$

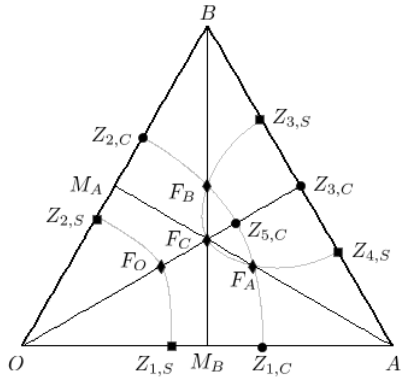

Point	$\mathbb{E}^2$	$\mathcal{F}$
$Z_{1,C}$	$\approx (0.6504, 0)$	$(u_{1,C}\,, \frac{u_{1,C}}{2})_{\mathcal{F}}$
$Z_{2,C}$	$\approx (0.3252, 0.5633)$	$(\frac{u_{1,C}}{2}\,, u_{1,C})_{\mathcal{F}}$
$Z_{3,C}$	$(\frac{3}{4}, \frac{\sqrt{3}}{4})$	$(\frac{1}{2}, \frac{1}{2})_{\mathcal{F}}$
$Z_{5,C}$	$\approx (0.5775, 0.3334)$	$(\frac{u_{5,C}}{2}\,, \frac{u_{5,C}}{2})_{\mathcal{F}}$
$Z_{1,S}$	$\approx (0.4034, 0)$	$(u_{1,S}\,, \frac{u_{1,S}}{2})_{\mathcal{F}}$
$Z_{2,S}$	$\approx (0.2017, 0.3494)$	$(\frac{u_{1,S}}{2}, u_{1,S})_{\mathcal{F}}$
$Z_{3,S}$	$\approx (0.6476, 0.6104)$	$(\frac{u_{2,S}}{2}, 1 - \frac{u_{2,S}}{2})_{\mathcal{F}}$
$Z_{4,S}$	$\approx (0.8524, 0.2507)$	$(\frac{u_{3,S}}{2}, 1 - \frac{u_{3,S}}{2})_{\mathcal{F}}$

Figure 7.3: Fixed points and critical zeros for $C_{1,3}$ and $S_{1,3}$

7.6 The nodal sets of $C_{1,3}$ and $S_{1,3}$

Properties 7.11 *Nodal sets of $C_{1,3}$ and $S_{1,3}$.*

1. *The function $C_{1,3}$ has only one critical zero $Z_{5,C}$ in the interior of the triangle. Its nodal set consists of the diagonal $[OM_O]$, and a regular arc from $Z_{1,C}$ to $Z_{2,C}$ which intersects $[OM_O]$ orthogonally at $Z_{5,C}$, and passes through F_A and F_B.*

2. *The function $S_{1,3}$ has no critical zero in the interior of the triangle. Its nodal set consists of two disjoint regular arcs, one from $Z_{1,S}$ to $Z_{2,S}$, passing through F_O; one from $Z_{3,S}$ to $Z_{4,S}$, passing through F_B and F_A.*

Proof. We have determined the common zeros of $C_{1,3}$ and $S_{1,3}$ located on the medians (Subsection 7.3), as well as the critical zeros on the open edges of the triangle $\mathcal{T}$ and on the medians $[OM]$ (Subsection 7.5). We already know the local behaviour at the vertices (Subsection 7.2). Using Subsection 7.4, we also know that the nodal set $N(C_{1,3})$ only meets the medians at the fixed points and at $Z_{5,C}$, and that the nodal set $N(S_{1,3})$ only meets the medians at the fixed points. Looking at the Taylor expansions, we can determine the local nodal patterns of $C_{1,3}$ and $S_{1,3}$ near the fixed points and near the critical zeros, see Figure 7.4. This figure also displays the medians, and takes into account the fact that $[OM_0] \subset N(C_{1,3})$.

The medians divide $\mathcal{T}$ into six isometric H-triangles, Figure 7.3. The nodal sets of $C_{1,3}$ and $S_{1,3}$ consist of finitely many nodal arcs which are smooth except at the critical zeros. They can only exit the interior of an H-triangle at a fixed point or at a critical zero, according to the local nodal patterns shown in Figure 7.4.

Claim. The functions $C_{1,3}$ and $S_{1,3}$ cannot have any critical zero in the interiors of the H-triangles.

Indeed, assume there is one critical zero Z in the interior of some H-triangle $\mathcal{H}$. At this point, the nodal set would consist of at least four semi-arcs. Following any such semi-arc,

we either obtain a simply closed nodal arc, or exit the triangle. Since there are at most three exit points (with only one exit direction at each point), there would be at least one simply closed nodal component in the interior of the triangle $\mathcal{H}$. This component would bound at least one nodal domain ω. The first Dirichlet eigenvalue $\lambda(\omega)$ would satisfy $\lambda(\omega) = \lambda_5(\mathcal{T}) = 13$. On the other-hand, since ω is contained in the interior of $\mathcal{H}$, we would have $\lambda(\omega) > \lambda(\mathcal{H}) = 21$ according to Lemma 7.4. This proves the claim by contradiction.

The last argument in the proof of the claim also shows that the interiors of the H-triangles cannot contain any closed nodal component. This shows that the nodal sets of $C_{1,3}$ and $S_{1,3}$ are indeed as shown in Figure 5.2. □

Remark.
Here is another argument to determine the nodal set $N(C_{1,3})$. The claim is that $C_{1,3}$ cannot have a second interior critical zero. Indeed, such a critical zero would be of order at least 2, and cannot belong to the median $[OM]$, so that it must belong to one of the two H-triangles determined by this median. For symmetry reasons, we would have at least one critical zero in each of these H-triangles. The eigenvalue $\lambda_5(\mathcal{T})$ which corresponds to the pairs $[1,3]$ and $[3,1]$ is also the second Dirichlet eigenvalue of these triangles, so that it has two nodal domains, Ω_1 and Ω_2. Applying the Euler formula [4, (2.11)] to the nodal partition $\mathcal{D} = (\Omega_1, \Omega_2)$, we would have

$$1 + \frac{1}{2}(1+1+2) \leq \chi(\frac{1}{2}\mathcal{T}) + \frac{1}{2}\sigma(\Omega_1, \Omega_2) = \chi(\Omega_1) + \chi(\Omega_2) \leq 2\,,$$

a contradiction.

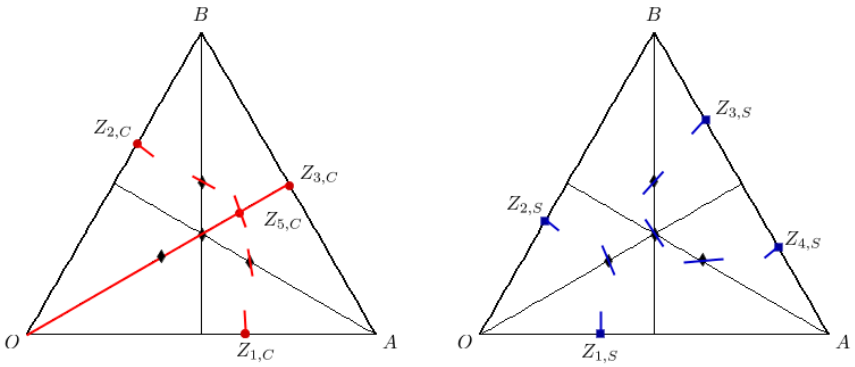

Figure 7.4: Local nodal patterns for $C_{1,3}$ (left) and $S_{1,3}$ (right)

7.7 Critical zeros of $\Psi^\theta_{1,3}$ on the sides of $\mathcal{T}$

As a consequence of Properties 7.6, the critical zeros of the functions $\Psi^\theta_{1,3}$, for $\theta \in]0, \frac{\pi}{6}]$, on the sides of the triangle $\mathcal{T}$ are determined by one of the equations

$$\cos\theta\, FC(u) \pm \sin\theta\, FS(u) = 0\,.$$

Since $\theta \in]0, \frac{\pi}{6}]$, the vertices of $\mathcal{T}$ are critical zeros of order 3 of $\Psi^\theta_{1,3}$ (Properties 7.1). Since we are interested in the critical zeros on the open edges, we can substitute FC, *resp.* FS, by the functions GC, *resp.* GS, defined as follows.

$$\begin{array}{ll} GC(u) & := \sin(\pi u)\,(cos(\pi u) - 1)\,(4\cos^2(\pi u) + 4\cos(\pi u) - 1)\ , \\ GS(u) & := 4\cos^4(\pi u) - \cos^2(\pi u) + \cos(\pi u) - 1\,. \end{array} \tag{7.20}$$

Properties 7.12 *The critical zeros of the function $\Psi^\theta_{1,3}$ on the open edges of the triangle $\mathcal{T}$ are determined by the following equations.*

1. *On the edge $[OA]$ parametrized by $u \mapsto (u, u/2)$,*

$$\cos\theta\, GC(u) + \sin\theta\, GS(u) = 0\,, \quad \textit{for } u \in [0, 2/3]\,. \tag{7.21}$$

2. *On the edge $[OB]$ parametrized by $u \mapsto (u/2, u)$,*

$$\cos\theta\, GC(u) - \sin\theta\, GS(u) = 0\,, \quad \textit{for } u \in [0, 2/3]\,. \tag{7.22}$$

3. *On the edge $[BA]$ parametrized by $u \mapsto (u/2, 1 - u/2)$,*

$$\cos\theta\, GC(u) - \sin\theta\, GS(u) = 0\,, \quad \textit{for } u \in [2/3, 4/3]\,. \tag{7.23}$$

For convenience, we introduce the functions,

$$H^\theta_\pm(u) = \cos\theta\, GC(u) \pm \sin\theta\, GS(u)\,. \tag{7.24}$$

Properties 7.13 *Recall the notation* (7.19).

1. *In the interval $]0, 2/3[$ (corresponding to critical zeros on the open side $[OA]$), the function H^θ_+ has two simple zeros,*

$$\beta_1(\theta) \in]0\,,\, u_{1,S}[\textit{ and } \beta_2(\theta) \in]u_{1,C}\,,\, \frac{2}{3}[\,.$$

   They are smooth increasing functions in θ.

2. *In the interval $]0\,,\, 2/3[$ (corresponding to critical zeros on the open side $[OB]$), the function H^θ_- has one simple zero*

$$\alpha_1(\theta) \in]\frac{1}{3}\,,\, u_{1,C}[\,.$$

   This is a smooth decreasing function of θ.

3. *In the interval* $]2/3, 4/3[$ *(corresponding to critical zeros on the open side* $[BA]$*), the function* H^θ_- *has one simple zero,*

$$\omega_1(\theta) \in]u_{2,S}\,,\, 1[\,.$$

This is a smooth decreasing function of θ*.*

Proof. Notice that the zeros of $H^\theta_\pm$ are continuous functions of θ because the equations $H^\theta_\pm(u) = 0$ can be written as polynomial equations in $\tan(\frac{\pi u}{2})$ with coefficients depending continuously on θ. We study the functions $H^\theta_\pm$ in the interval $]-1/6, 3/2[$ which contains the interval $[0, 4/3]$.

First of all, taking into account the fact that $\theta \in]0, \pi/6]$, we look at the values of the functions $H^\theta_\pm$ at the points

$$0 < u_{1,S} < \frac{1}{3} < u_{1,C} < \frac{2}{3} < u_{2,S} < 1 < u_{3,S} < \frac{4}{3}\,,$$

and infer the existence of at least one zero in each of the intervals mentioned in the statements. Note that the zero $\beta_1(\theta)$ comes from the fact that the vertex O has order 6 for $C_{1,3}$ and order 3 for $\Psi^\theta_{1,3}$ as soon as $0 < \theta \leq \pi/6$. The details appear in Table 7.1 (in which we have only indicated the useful values). The values listed above correspond to the vertices of the triangles ($0, \frac{2}{3}$ and $\frac{4}{3}$), the mid-points on the edges ($\frac{1}{3}$ and 1), and the critical zeros on the open edges.

We then investigate whether the zeros of $H^\theta_\pm$ can have order at least 2. More precisely, we investigate whether there exists a pair (θ, u) such that

$$\begin{array}{l} \cos\theta\, GC(u) \pm \sin\theta\, GS(u) = 0\,, \\ \cos\theta\, GC'(u) \pm \sin\theta\, GS'(u) = 0\,. \end{array} \tag{7.25}$$

For this purpose, we define the function

$$WCS(u) := GC(u)GS'(u) - GS(u)GC'(u). \tag{7.26}$$

Lemma 7.14 *The function* WCS *satisfies the relation*

$$WCS(u) = \pi\,(1 - \cos(\pi u))\,(2\cos(\pi u) + 1)^2\,\left(13\cos^3(\pi u) - 9\cos(\pi u) + 4\right)\,. \tag{7.27}$$

Furthermore, the function WCS *is non-negative, and vanishes in the interval* $]-1/6, 3/2[$ *if and only if* $u \in \{0, \frac{2}{3}, \frac{4}{3}\}$.

Proof of the Lemma. Compute the derivatives, make use of the Chebyshev polynomials, and notice that the polynomial of degree 3 in $\cos(\pi u)$ is always bigger than or equal to 1. □

Lemma 7.14 implies that for $\theta \in]0, \pi/6]$, the zeros of the functions $H^\theta_\pm$ in the interval $]0, \frac{2}{3}[$ and $]\frac{2}{3}, \frac{4}{3}[$ are simple, so that they are smooth in θ. If $u(\theta)$ is such a zero, its derivative with respect to θ satisfies the relation

$$1 + \tan^2(\theta) = \pm\frac{WCS(u(\theta))}{GS^2(u(\theta))}u'(\theta)\,.$$

$u \in [0,4/3]$	$GC(u)$	$GS(u)$	$H^\theta_+(u)$	$H^\theta_1(u)$
0	0	3	$3\sin\theta$	$-3\sin\theta$
$\beta_1(\theta)$	–	–	0	–
$u_{1,S}$ ≈ 0.2689	$GC(u_{1,S})$ ≈ -0.8660	0	$GC(u_{1,S})\cos\theta$ $\approx -0.8660\cos\theta$	$GC(u_{1,S})\cos\theta$ $\approx -0.8660\cos\theta$
$\frac{1}{3}$	$GC(\frac{1}{3}) = -\frac{\sqrt{3}}{2}$ ≈ -0.866025	$GS(\frac{1}{3}) = -\frac{1}{2}$	$-\cos(\theta - \frac{\pi}{6})$	$-\cos(\theta + \frac{\pi}{6})$
$\alpha_1(\theta)$	–	–	–	0
$u_{1,C}$ ≈ 0.4336	0	$GS(u_{1,C})$ ≈ -0.8284	$GS(u_{1,C})\sin\theta$ $\approx -0.8284\sin\theta$	$-GS(u_{1,C})\sin\theta$ $\approx 0.8284\sin\theta$
$\beta_2(\theta)$	–	–	0	–
$\frac{2}{3}$	$GC(\frac{2}{3}) = \frac{3\sqrt{3}}{2}$ ≈ 2.5981	$GS(\frac{2}{3}) = -\frac{3}{2}$	$3\cos(\theta + \frac{\pi}{6})$	$3\cos(\theta - \frac{\pi}{6})$
$u_{2,S}$ ≈ 0.8635	$GC(u_{2,S})$ ≈ 1.0554	0	– –	$GC(u_{2,S})\cos\theta$ $\approx 1.0554\cos\theta$
$\omega_1(\theta)$	–	–	–	0
1	0	1	–	$-\sin\theta$
$u_{3,S}$ 1.1365	$GC(u_{3,S})$ ≈ -1.0554	0	– –	$GC(u_{3,S})\cos\theta$ $\approx -1.0554\cos\theta$
$\frac{4}{3}$	$GC(\frac{4}{3}) = -\frac{3\sqrt{3}}{3}$ ≈ -2.5981	$GS(\frac{4}{3}) = -\frac{3}{2}$	– –	$-3\cos(\theta + \frac{\pi}{6})$

Table 7.1: Values of $H^\theta_\pm$

We can now start from the function $\Psi^{\frac{\pi}{6}}_{1,3} = -S_B$, and follow the zeros by continuity, using Corollary 7.10. This proves Properties 7.13. □

Recall the notation of Corollary 7.10.

Corollary 7.15 *Critical zeros of the function $\Psi^\theta_{1,3}$ for $\theta \in]0, \frac{\pi}{6}]$.*

1. *There are two critical zeros of order 2 on the side $[OA]$, one $Z_{4,\theta}$ in the segment $]O, Z_{4,S_B}]$, and one $Z_{3,\theta}$ in the segment $]Z_{1,C}, Z_{3,S_B}]$.*
2. *There is one critical zero $Z_{1,\theta}$ of order 2 on the segment $[Z_{1,S_B}, Z_{2,C}[$.*
3. *There is one critical zero $Z_{2,\theta}$ of order 2 on the segment $[Z_{2,S_B}, Z_{3,C}[$ (recall that $Z_{3,C} = M_O$).*

7.8 Nodal set of $\Psi^\theta_{1,3}$

Proposition 7.16 *For $\theta \in]0, \frac{\pi}{6}]$ the nodal set of $\Psi^\theta_{1,3}$ consists of two disjoint simple arcs, one from $Z_{1,\theta}$ to $Z_{2,\theta}$, through F_B; another from $Z_{4,\theta}$ to $Z_{3,\theta}$, through the points $\{F_0, F_C$ and $F_A\}$. In particular, the function $\Psi^\theta_{1,3}$ has three nodal domains. As a consequence, the eigenvalue $\lambda_5(\mathcal{T}) = 13$ is not Courant-sharp.*

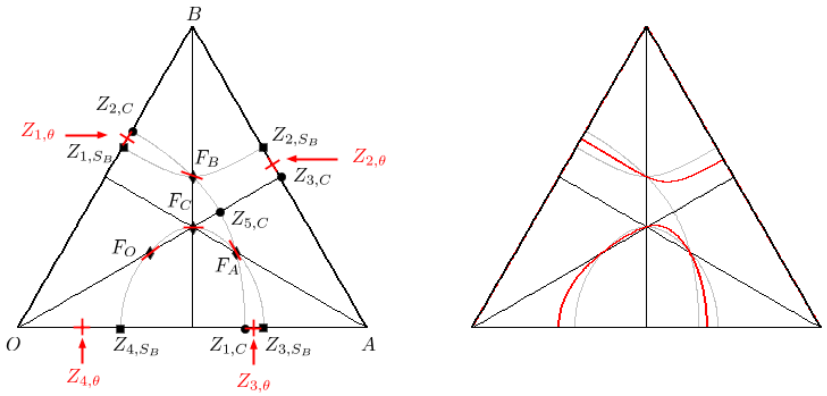

Figure 7.5: Nodal patterns and nodal set for $\Psi^{\theta}_{1,3}$

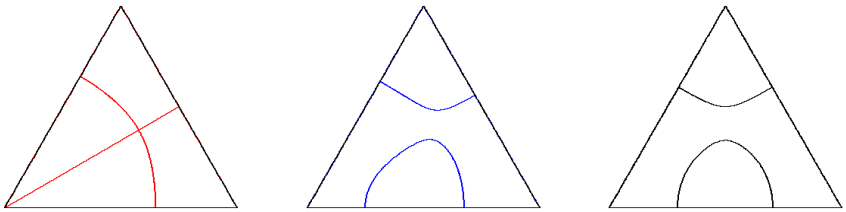

Figure 7.6: Nodal set of $\Psi^{\theta}_{1,3}$, for $\theta = 0\,,\ \frac{\pi}{12}$ and $\frac{\pi}{6}$

Proof. It is similar to the proof of Properties 7.11, and illustrated by Figure 7.5. The picture on the left-hand side displays the local nodal patterns, from which we can deduce that there are no interior critical zeros in any of the six H-triangles determined by the medians. The picture on the right-hand side displays the nodal set $N(\Psi^{\frac{\pi}{12}}_{1,3})$ computed with Maple. The pictures in Figure 7.6 show the nodal sets of the eigenfunctions $C_{1,3}$, $\Psi^{\frac{\pi}{12}}_{1,3}$ and $\Psi^{\frac{\pi}{6}}_{1,3}$ (from left to right). □

Remark. Let Ψ be an eigenfunction. Once one knows the critical zeros of Ψ, together with their orders, and the number of connected components of $N(\Psi)\cup\partial\mathcal{T}$, one can apply the Euler-type formula of [10, Proposition 2.8] to obtain the number of nodal domains of Ψ. Using the proof of Proposition 7.16 and this formula, one can recover the number of nodal domains of $\Psi^{\theta}_{1,3}$: three for any $\theta \in]0, \frac{\pi}{6}]$.

8 The eigenvalue $\lambda_7(\mathcal{T})$ and its eigenspace

We call $\mathcal{E}_7$ the 2-dimensional eigenspace associated with the eigenvalue $\lambda_7(\mathcal{T})$, i.e., with the pairs $[2,3]$ and $[3,2]$. Recall the eigenfunctions,

$$\begin{aligned} C_{2,3}(s,t) = \;& \cos 2\pi(2s+3t) - \cos 2\pi(-2s+5t) - \cos 2\pi(5s-3t) \\ & - \cos 2\pi(-3s-2t) + \cos 2\pi(3s-5t) + \cos 2\pi(-5s+2t)\,, \\ S_{2,3}(s,t) = \;& \sin 2\pi(2s+3t) - \sin 2\pi(-2s+5t) - \sin 2\pi(5s-3t) \\ & - \sin 2\pi(-3s-2t) + \sin 2\pi(3s-5t) + \sin 2\pi(-5s+2t)\,. \end{aligned} \tag{8.1}$$

In this section, we give a careful analysis of the zero set of the family $\Psi^\theta_{2,3}$. Our aim is to show that none of these eigenfunctions has 7 nodal domains.

8.1 Symmetries

Taking Subsection 4.2 into account, we find that

$$\begin{aligned} \sigma_1^*\Psi^\theta_{2,3} &= \Psi^{\pi-\theta}_{2,3}\,, \\ \sigma_2^*\Psi^\theta_{2,3} &= \Psi^{\frac{5\pi}{3}-\theta}_{2,3}\,, \\ \sigma_3^*\Psi^\theta_{2,3} &= \Psi^{\frac{\pi}{3}-\theta}_{2,3}\,, \\ (\sigma_2\circ\sigma_1)^*\Psi^\theta_{2,3} &= \Psi^{\frac{4\pi}{3}+\theta}_{2,3}\,, \\ (\sigma_1\circ\sigma_2)^*\Psi^\theta_{2,3} &= \Psi^{\frac{2\pi}{3}+\theta}_{2,3}\,. \end{aligned} \tag{8.2}$$

It follows that, up to multiplication by scalars, and for $V \in \{O, A, B\}$, the eigenspace $\mathcal{E}_7$ contains a unique eigenfunction S_V, *resp.* a unique eigenfunction C_V, which is invariant, *resp.* anti-invariant, under the symmetry $\sigma_{i(V)}$ with respect to the median $[VM]$ issued from the vertex V, where $i(O) = 1, i(A) = 3$, and $i(B) = 2$. More precisely, we have

$$\begin{aligned} &S_O = \Psi^{\frac{\pi}{2}}_{2,3} \text{ and } C_O = \Psi^0_{2,3}\,, \\ &S_A = \Psi^{\frac{7\pi}{6}}_{2,3} \text{ and } C_A = \Psi^{\frac{2\pi}{3}}_{2,3}\,, \\ &S_B = \Psi^{\frac{11\pi}{6}}_{2,3} \text{ and } C_B = \Psi^{\frac{4\pi}{3}}_{2,3}\,. \end{aligned} \tag{8.3}$$

Note that C_O, *resp.* S_O, are the functions $C_{2,3}$, *resp.* $S_{2,3}$, and that,

$$\begin{aligned} &S_A = \rho_-^* S_O \text{ and } C_A = \rho_-^* C_O\,, \\ &S_B = \rho_+^* S_O \text{ and } C_B = \rho_+^* C_O\,. \end{aligned} \tag{8.4}$$

The eigenfunctions S_V, *resp.* C_V, are permuted under the action of the rotations $\rho_+ = \sigma_2 \circ \sigma_1$ and $\rho_- = \sigma_1 \circ \sigma_2$. The eigenspace $\mathcal{E}_7$ does not contain any non trivial rotation invariant eigenfunction.

Since $\Psi_{2,3}^{\theta+\pi} = -\Psi_{2,3}^{\theta}$, it follows from (8.2) that, up to the symmetries σ_i, the nodal sets of the family $\Psi_{2,3}^{\theta}$, $\theta \in [0, 2\pi]$ are determined by the nodal sets of the sub-family $\theta \in [0, \frac{\pi}{6}]$.

From now on, we assume that $\theta \in [0, \frac{\pi}{6}]$.

8.2 Behaviour at the vertices

The vertices of the equilateral triangle $\mathcal{T}$ belong to the nodal set $N(\Psi_{2,3}^{\theta})$ for all θ. For geometric reasons, the order of vanishing at a vertex is at least 3. More precisely,

Properties 8.1 *Behaviour of $\Psi_{2,3}^{\theta}$ at the vertices.*

1. *The function $\Psi_{2,3}^{\theta}$ vanishes at order 6 at O if and only if $\theta \equiv 0 \pmod{\pi}$; otherwise it vanishes at order 3.*
2. *The function $\Psi_{2,3}^{\theta}$ vanishes at order 6 at A if and only if $\theta \equiv \frac{2\pi}{3} \pmod{\pi}$; otherwise it vanishes at order 3.*
3. *The function $\Psi_{2,3}^{\theta}$ vanishes at order 6 at B if and only if $\theta \equiv \frac{4\pi}{3} \pmod{\pi}$; otherwise it vanishes at order 3.*

In other words, up to scaling, the only eigenfunction $\Psi_{2,3}^{\theta}$ which vanishes at higher order at a vertex $V \in \{O, A, B\}$ is C_V, the anti-invariant eigenfunction with respect to the median issued from the vertex V. In particular, when $\theta \in]0, \frac{\pi}{6}]$, the three vertices are critical zeros of order three for the eigenfunction $\Psi_{2,3}^{\theta}$, and no interior nodal curve of such an eigenfunction can arrive at a vertex.

Proof. Compute the Taylor expansions of $\Psi_{2,3}^{\theta}$ at the points under consideration, and use (8.3). □

8.3 Fixed points on the medians

Since the median $[OM]$ is contained in the nodal set $N(C_{2,3})$, the intersection points of $[OM]$ with $N(S_{2,3})$ are fixed points of the family $N(\Phi_{2,3}^{\theta})$, i.e., common zeros of the functions $\Psi_{2,3}^{\theta}$. If we parametrize $[OM]$ by $u \mapsto (u, u)$ with $u \in [0, \frac{1}{2}]$, we find that

$$S_{2,3}\big|_{[OM]}(u) = 2\sin(10\pi u) - 2\sin(6\pi u) - 2\sin(4\pi u). \tag{8.5}$$

This function can be factored as,

$$S_{2,3}\big|_{[OM]}(u) \;\; = -8\sin(2\pi u)\,\sin(3\pi u)\,\sin(5\pi u)\,. \tag{8.6}$$

This formula shows that there are three fixed points on the open median $[OM]$, the centroid of the triangle $F_C = (\frac{1}{3}, \frac{1}{3})_{\mathcal{F}}$, the point $F_{1,O} = (\frac{1}{5}, \frac{1}{5})_{\mathcal{F}}$ and the point $F_{2,O} = (\frac{2}{5}, \frac{2}{5})_{\mathcal{F}}$. The points O and M_O are "obvious" fixed points (corresponding to the values 0 and 1/2).

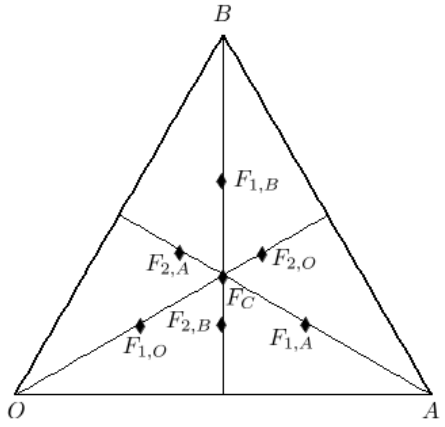

Point	$\mathbb{E}^2$	$\mathcal{F}$
Vertex O	$(0,0)$	$(0,0)_{\mathcal{F}}$
Vertex A	$(1,0)$	$(\frac{2}{3},\frac{1}{3})_{\mathcal{F}}$
Vertex B	$(\frac{1}{2},\frac{\sqrt{3}}{2})$	$(\frac{1}{3},\frac{2}{3})_{\mathcal{F}}$
Fixed point F_C	$(\frac{1}{2},\frac{\sqrt{3}}{6})$	$(\frac{1}{3},\frac{1}{3})_{\mathcal{F}}$
Fixed point $F_{1,O}$	$(\frac{3}{10},\frac{\sqrt{3}}{10})$	$(\frac{1}{5},\frac{1}{5})_{\mathcal{F}}$
Fixed point $F_{2,O}$	$(\frac{3}{5},\frac{\sqrt{3}}{5})$	$(\frac{2}{5},\frac{2}{5})_{\mathcal{F}}$
Fixed point $F_{1,A}$	$(\frac{7}{10},\frac{\sqrt{3}}{10})$	$(\frac{7}{15},\frac{1}{3})_{\mathcal{F}}$
Fixed point $F_{2,A}$	$(\frac{2}{5},\frac{\sqrt{3}}{5})$	$(\frac{4}{15},\frac{1}{3})_{\mathcal{F}}$
Fixed point $F_{1,B}$	$(\frac{1}{2},\frac{3\sqrt{3}}{10})$	$(\frac{1}{3},\frac{7}{15})_{\mathcal{F}}$
Fixed point $F_{2,B}$	$(\frac{1}{2},\frac{\sqrt{3}}{10})$	$(\frac{1}{3},\frac{4}{15})_{\mathcal{F}}$

Figure 8.1: Fixed points for $N(\Psi^{\theta}_{2,3})$

Taking into account the action of $G_{\mathcal{T}}$ on the space $\mathcal{E}_7$, see (8.2)-(8.4), we infer that the points $F_{1,A} = (\frac{7}{15},\frac{1}{3})_{\mathcal{F}}$, $F_{2,A} = (\frac{4}{15},\frac{1}{3})_{\mathcal{F}}$, $F_{1,B} = (\frac{1}{3},\frac{7}{15})_{\mathcal{F}}$, and $F_{2,B} = (\frac{1}{3},\frac{4}{15})_{\mathcal{F}}$, are also common zeros for the family $\Psi^{\theta}_{2,3}$. They are deduced from $F_{i,O}$ by applying the rotations $\rho_{\pm}$, and situated on the two other medians.

Using Taylor expansions, it is easy to check that the fixed points F_* are not critical zeros of the functions $\Psi^{\theta}_{2,3}$. In the neighborhood of the fixed points F_*, the nodal set consists of a single regular arc.

Remark. Note that we do not claim to have determined all the fixed points of the family $N(\Psi^{\theta}_{2,3})$ i.e., the set $N(C_{2,3}) \cap N(S_{2,3})$. We have only determined the fixed points located on the medians.

8.4 Partial barriers for the nodal sets

We have seen that the family $\Psi^{\theta}_{2,3}$ has seven fixed points, the centroid F_C of the triangle, and six other points $F_{1,O}$, $F_{2,O}$, $F_{1,A}$, $F_{2,A}$, $F_{1,B}$ and $F_{2,B}$, located respectively on the open medians $[OM]$, $[AM]$, and $[BM]$, see Figure 8.1.

For $0 \leq a \leq 1$, let D_a denote the line whose equation in the parametrization $\mathcal{F}$ is $s+t = a$.

In this section, we investigate the intersections of the nodal sets with the medians, and with the lines D_a for $a \in \{\frac{2}{5},\frac{3}{5},\frac{2}{3},\frac{4}{5}\}$ i.e., the lines through the fixed points, parallel to the edge $[BA]$.

Lemma 8.2 *For any θ, the nodal set $N(\Psi^{\theta}_{2,3})$ intersects each median at exactly three points unless the function $\Psi^{\theta}_{2,3}$ is one of the functions C_V for $V \in \{O, A, B\}$, in which*

case the corresponding median is contained in the nodal set. In particular, if $\theta \in]0, \frac{\pi}{6}]$, *the nodal set* $N(\Psi^{\theta}_{2,3})$ *only meets the medians at the fixed points* $\{F_{i,O}, F_{i,A}, F_{i,B}, F_C\}$, *for* $i = 1, 2$.

Proof. Use the following facts:
(i) the families $\{C_O, S_O\}$, $\{C_A, S_A\}$ and $\{C_B, S_B\}$ span $\mathcal{E}_7$;
(ii) the function C_V vanishes on the median issued from the vertex V.
Then write $\Psi^{\theta}_{2,3} = \alpha C_V + \beta S_V$. If $x \in [VM] \cap N(\Psi^{\theta}_{2,3})$, then $\beta S_V(x) = 0$. If $\beta \neq 0$, then $x \in \{F_C, F_{1,V}, F_{2,V}\}$. If $\beta = 0$, then $[VM] \subset N(\Psi^{\theta}_{2,3})$. □

Remark. A consequence of Lemma 8.2 and Subsection 8.3 is that for if $\theta \in]0, \frac{\pi}{6}]$, no critical zero of the function $\Psi^{\theta}_{2,3}$ can occur on the medians.

Lemma 8.3 *The intersections of the lines* D_a *for* $a \in \{\frac{2}{5}, \frac{3}{5}, \frac{2}{3}, \frac{4}{5}\}$ *with the nodal sets* $N(C_{2,3})$ *and* $N(S_{2,3})$ *are as follows,*

$$\begin{array}{lll} D_{\frac{2}{5}} \cap N(C_{2,3}) = \{F_{1,O}\}, & \textit{and} & D_{\frac{2}{5}} \cap N(S_{2,3}) = \{F_{1,O}\}, \\ D_{\frac{3}{5}} \cap N(C_{2,3}) = \{G_O, F_{2,A}, F_{2,B}\}, & \textit{and} & D_{\frac{3}{5}} \cap N(S_{2,3}) = \{F_{2,A}, F_{2,B}\}, \\ D_{\frac{2}{3}} \cap N(C_{2,3}) = \{F_C, G_A, G_B\}, & \textit{and} & D_{\frac{2}{3}} \cap N(S_{2,3}) = \{F_C\}, \\ D_{\frac{4}{5}} \cap N(C_{2,3}) = \{F_{2,O}, F_{1,A}, F_{1,B}\}, & \textit{and} & D_{\frac{4}{5}} \cap N(S_{2,3}) = \{F_{2,O}, F_{1,A}, F_{1,B}\}, \end{array} \tag{8.7}$$

where G_A *and* G_B *are symmetrical with respect to* $[OM]$, *and* $G_O = (0.3, 0.3)_{\mathcal{F}}$. *These lines are tangent to* $N(S_{2,3})$ *at the points* $F_{1,O}, F_C$ *and* $F_{2,O}$.

Proof. The segment $D_a \cap \mathcal{T}$ is parametrized by $u \mapsto (u, a-u)$ for $u \in [\frac{a}{3}, \frac{2a}{3}]$. For each value $a \in \{\frac{2}{5}, \frac{3}{5}, \frac{2}{3}, \frac{4}{5}\}$, define

$$\begin{array}{l} BC_a(u) = C_{2,3}(u, a-u), \quad u \in [\frac{a}{3}, \frac{2a}{3}]\,, \\ BS_a(u) = S_{2,3}(u, a-u), \quad u \in [\frac{a}{3}, \frac{2a}{3}]\,. \end{array} \tag{8.8}$$

Taking $a = \frac{2}{5}$, we find

$$\begin{array}{l} BC_{\frac{2}{5}}(u) = -\cos(14\pi u) + \cos(14\pi u + 2\pi/5) + \cos(16\pi u) - \cos(16\pi u + 3\pi/5)\,, \\ BS_{\frac{2}{5}}(u) = \sin(14\pi u) - \sin(14\pi u + 2\pi/5) + \sin(16\pi u) + \sin(16\pi u - 2\pi/5)\,. \end{array} \tag{8.9}$$

These equations simplify to

$$\begin{array}{l} BC_{\frac{2}{5}}(u) = -4\sin(\pi/5)\sin(15\pi u)\sin(\pi u + 3\pi/10)\,, \\ BS_{\frac{2}{5}}(u) = 4\sin(\pi/5)\sin(15\pi u)\cos(\pi u + 3\pi/10)\,. \end{array} \tag{8.10}$$

Similarly, we obtain

$$\begin{array}{l} BC_{\frac{3}{5}}(u) = 4\sin(\pi/5)\sin(15\pi u)\cos(\pi u + \pi/5)\,, \\ BS_{\frac{3}{5}}(u) = 4\sin(\pi/5)\sin(15\pi u)\sin(\pi u + \pi/5)\,. \end{array} \tag{8.11}$$

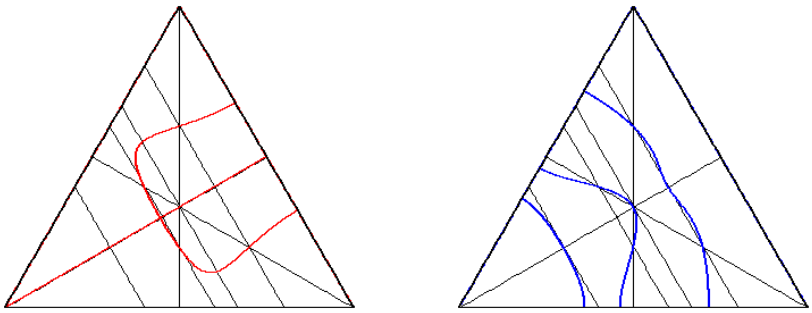

Figure 8.2: Partial barriers for $N(C_{2,3})$ and $N(S_{2,3})$

$$\begin{aligned} BC_{\frac{2}{3}}(u) &= 2\sqrt{3}\sin(9\pi u)\cos(7\pi u - \pi/3)\,, \\ BS_{\frac{2}{3}}(u) &= 2\sqrt{3}\sin(9\pi u)\sin(7\pi u - \pi/3)\,. \end{aligned} \tag{8.12}$$

$$\begin{aligned} BC_{\frac{4}{5}}(u) &= -4\cos(\pi/10)\sin(15\pi u)\sin(\pi u + \pi/10)\,, \\ BS_{\frac{4}{5}}(u) &= 4\cos(\pi/10)\sin(15\pi u)\cos(\pi u + \pi/10)\,. \end{aligned} \tag{8.13}$$

Looking at the zeros of the above functions in the respective intervals, the lemma follows. □

The lemmas are illustrated by Figure 8.2. It displays the partial barriers (thin segments), and the nodal sets as computed by Maple (thicker lines).

8.5 Critical zeros of $C_{2,3}$ and $S_{2,3}$ on the sides of $\mathcal{T}$, and on the median $[OM]$

Define the functions

$$\begin{aligned} FC(u) &:= -2\sin(8\pi u) + 3\sin(7\pi u) - 5\sin(\pi u)\,, \\ FS(u) &:= -2\cos(8\pi u) - 3\cos(7\pi u) + 5\cos(\pi u)\,. \end{aligned} \tag{8.14}$$

Properties 8.4 *The partial derivatives of the functions $C_{2,3}$ and $S_{2,3}$ satisfy the following relations.*

1. *Parametrize the edge $[OA]$ by $u \mapsto (u, u/2)$, with $u \in [0, 2/3]$. Then,*

$$\begin{aligned} \partial_s C_{2,3}(u, u/2) &= 2\pi FC(u), \quad \partial_t C_{2,3}(u, u/2) = -4\pi FC(u)\,, \\ \partial_s S_{2,3}(u, u/2) &= 2\pi FS(u), \quad \partial_t S_{2,3}(u, u/2) = -4\pi FS(u)\,. \end{aligned} \tag{8.15}$$

2. *Parametrize the edge $[OB]$ by $u \mapsto (u/2, u)$, with $u \in [0, 2/3]$. Then,*

$$\begin{aligned} \partial_s C_{2,3}(u/2, u) &= 4\pi FC(u), \quad \partial_t C_{2,3}(u/2, u) = -2\pi FC(u)\,, \\ \partial_s S_{2,3}(u/2, u) &= -4\pi FS(u), \quad \partial_t S_{2,3}(u/2, u) = 2\pi FS(u)\,. \end{aligned} \tag{8.16}$$

3. Parametrize the edge $[BA]$ by $u \mapsto (u/2, 1-u/2)$, with $u \in [2/3, 4/3]$. Then,

$$\begin{array}{l} \partial_s C_{2,3}(u/2, 1-u/2) = -2\pi FC(u), \quad \partial_t C_{2,3}(u/2, 1-u/2) = -2\pi FC(u)\,, \\ \partial_s S_{2,3}(u/2, 1-u/2) = 2\pi FS(u), \quad \partial_t S_{2,3}(u/2, 1-u/2) = 2\pi FS(u)\,. \end{array} \tag{8.17}$$

As a consequence, the critical zeros of $C_{2,3}$ and $S_{2,3}$ on the edges $[OA]$ and $[OB]$, resp. *on the edge $[BA]$, are determined by the zeros of FC and FS in the intervals $[0, 2/3]$,* resp. $[2/3, 4/3]$.

Proof. It suffices to compute the partial derivatives of $C_{2,3}$ and $S_{2,3}$, and to make the substitutions corresponding to the parametrization of the edges. □

Define the polynomials

$$\begin{array}{ll} P_C(x) & := 8x^3 + 2x^2 - 4x + 1\,, \\ P_S(x) & := 8x^5 + 6x^4 - 10x^3 - 4x^2 + 4x - \frac{1}{4}\,. \end{array} \tag{8.18}$$

Lemma 8.5 *The functions FC and FS satisfy,*

$$\begin{array}{ll} FC(u) & = -8\sin(\pi u)\left(\cos(\pi u) - 1\right)^2 \left(2\cos(\pi u) + 1\right)^2 \, P_C\left(\cos(\pi u)\right)\,, \\ FS(u) & = -8\left(\cos(\pi u) - 1\right)\left(2\cos(\pi u) + 1\right)^2 \, P_S\left(\cos(\pi u)\right)\,. \end{array} \tag{8.19}$$

Proof. Use the Chebyshev polynomials. □

Lemma 8.6 *Roots of the polynomials P_C and P_S.*

1. *The polynomial P_C has one root $-\xi_1 \in [-1, 1]$, where $\xi_1 \approx 0.9311441818$.*
2. *The polynomial P_S has three roots in the interval $[-1, 1]$,*

$$\eta_1 \approx 0.7261887036\,,\ \eta_2 \approx 0.5658979255\,,\ \textit{and}\ \eta_3 \approx 0.06784981490\,.$$

Define the numbers

$$\begin{array}{l} u_{1,C} := 1 - \frac{\arccos \xi_1}{\pi} \approx 0.8811882234\,, \\ u_{2,C} := 1\,, \\ u_{3,C} := 1 + \frac{\arccos \xi_1}{\pi} \approx 1.1188117766\,, \\ u_{1,S} := \frac{\arccos \eta_1}{\pi} \approx 0.2412898667\,, \\ u_{2,S} := \frac{\arccos \eta_2}{\pi} \approx 0.3085296215\,, \\ u_{3,S} := \frac{\arccos \eta_3}{\pi} \approx 0.4783861278\,. \end{array} \tag{8.20}$$

In the interval $[0, 4/3]$, the function FC vanishes at $0, 2/3$ and $4/3$ (these values of u correspond to the vertices), and at the $u_{i,C}$ which correspond to critical zeros $Z_{i,C}$ of $C_{2,3}$ on the edge $[BA]$. In the interval $[0, 4/3]$, the function FS vanishes at $0, 2/3$ and $4/3$ (these values of u correspond to the vertices), and at the $u_{i,S}$ which correspond to critical zeros $Z_{i,S}$ of $S_{2,3}$ on the edge $[OA]$, and $Z_{i+3,S}$ on the edge $[OB]$.

Properties 8.7 *Critical zeros of the functions $C_{2,3}$ and $S_{2,3}$ on the open edges of $\mathcal{T}$.*

1. *The function $C_{2,3}$ has three critical zeros of order 2 on the open edge $[BA]$: $Z_{1,C}$ between B and M_O, $Z_{2,C} = M_O$, and $Z_{3,C}$ between M_O and A. It has no critical zero on the open edges $[OA]$ and $[OB]$.*

2. *The function $S_{2,3}$ has three critical zeros of order 2 on the open edge $[OA]$: $Z_{i,S}$, for $i \in \{1,2,3\}$. The points $Z_{1,S}$ and $Z_{2,S}$ lie between O and M_B; the point $Z_{3,S}$ between M_B and A. The function $S_{2,3}$ has three critical zeros of order 2 on the open edge $[OB]$, $Z_{i+3,S}$ for $i \in \{1,2,3\}$, where $Z_{i,S}$ and $Z_{i+3,S}$ are symmetric with respect to the median $[OM]$. The function $S_{2,3}$ has no critical zero on the open edge $[BA]$.*

Proof. Use Properties 8.4 and Lemma 8.6. □

Remark. The vertex O is a critical zero of order 6 of $C_{2,3}$, and a critical zero of order 3 of $S_{2,3}$. The vertices A and B are critical zeros of order 3 of both $C_{2,3}$ and $S_{2,3}$, see Properties 8.1.

Properties 8.8 *Critical zeros of the functions $C_{2,3}$ and $S_{2,3}$ on the median $[OM]$.*

1. *The function $C_{2,3}$ has one critical zero at O of order 6; two critical zeros of order 2, $M_O = Z_{2,C}$ and $Z_{5,C}$, corresponding to*

$$u_{5,C} := 1 - \arccos(1 - 1/\sqrt{2})/\pi \approx 0.5946180472\,.$$

2. *The function $S_{2,3}$ has no critical zero on the median $[OM]$, except the point O.*

Proof. Since $C_{2,3}$ vanishes on the median, its critical zeros on the median are the common zeros of its partial derivatives. They are precisely the zeros of the function

$$\sin(5\pi u) - 7\sin(3\pi u) + 8\sin(2\pi u)\,,$$

if we parametrize the median by $u \mapsto (u/2, u/2)$ for $u \in [0,1]$. The above function can be factorized as

$$8\sin(\pi u)\big(\cos(\pi u) - 1\big)^2\big(2\cos^2(\pi u) + 4\cos(\pi u) + 1\big)\,,$$

and the first assertion follows.

For the second assertion, we have to look for the common zeros of the function $S_{2,3}$ and its derivatives on the median. This amounts to finding the common zeros of the functions

$$\sin(5\pi u) - \sin(3\pi u) - \sin(2\pi u)\,,$$

and

$$5\cos(5\pi u) - 3\cos(3\pi u) - 2\cos(2\pi u)\,,$$

in the interval $[0,1]$. The first function can be factorized as

$$-4\sin(\frac{5\pi}{2}u)\sin(\frac{3\pi}{2}u)\sin(\pi u)\,,$$

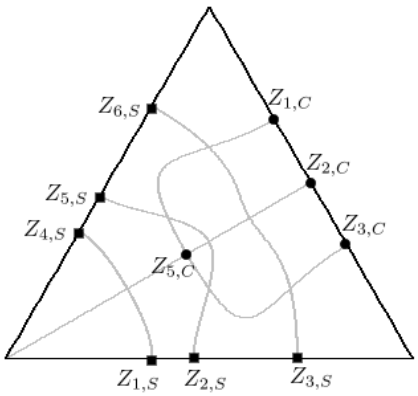

Point	$\mathbb{E}^2$	$\mathcal{F}$
$Z_{1,C}$	$\approx (0.6609, 0.5873)$	$(\frac{u_{1,C}}{2}, 1-\frac{u_{1,C}}{2})_{\mathcal{F}}$
$Z_{2,C}$	$\approx (0.75, 0.4330)$	$(\frac{1}{2}, \frac{1}{2})_{\mathcal{F}}$
$Z_{3,C}$	$\approx (0.8391, 0.2787)$	$(\frac{u_{3,C}}{2}, 1-\frac{u_{3,C}}{2})_{\mathcal{F}}$
$Z_{5,C}$	$\approx (0.4459, 0.2576)$	$(\frac{u_{5,C}}{2}, \frac{u_{5,C}}{2})_{\mathcal{F}}$
$Z_{1,S}$	$\approx (0.3619, 0)$	$(u_{1,S}, \frac{u_{1,S}}{2})_{\mathcal{F}}$
$Z_{2,S}$	$\approx (0.4628, 0)$	$(u_{2,S}, \frac{u_{2,S}}{2})_{\mathcal{F}}$
$Z_{3,S}$	$\approx (0.7176, 0)$	$(u_{3,S}, \frac{u_{3,S}}{2})_{\mathcal{F}}$
$Z_{4,S}$	$\approx (0.1810, 0.3135)$	$(\frac{u_{1,S}}{2}, u_{1,S})_{\mathcal{F}}$
$Z_{5,S}$	$\approx (0.2314, 0.4008)$	$(\frac{u_{2,S}}{2}, u_{2,S})_{\mathcal{F}}$
$Z_{6,S}$	$\approx (0.3588, 0.6215)$	$(\frac{u_{3,S}}{2}, u_{3,S})_{\mathcal{F}}$

Figure 8.3: Critical zeros of $C_{2,3}$ and $S_{2,3}$

and it is easy to check that the only common zero is $u = 0$. □

Figure 8.3 displays the critical zeros of $C_{2,3}$ and $S_{2,3}$ (the nodal sets computed with Maple appear in grey).

In view of later reference, we mention the following corollary of Properties 8.8.

Recall (see the notation (8.3)) that $\Psi_{2,3}^{\frac{11\pi}{6}} = -S_A$, and that $S_A = \rho_-^* S_O$.

Corollary 8.9 *Critical zeros of the function S_A.*

1. *The function S_A has three critical zeros of order 2 on the open side $[OA]$, $Z_{i,S_A} = \rho_+(Z_{i,S})$ for $i \in \{4,5,6\}$.*
2. *The function S_A has three critical zeros of order 2 on the open side $[BA]$, $Z_{i,S_A} = \rho_+(Z_{i,S})$ for $i \in \{1,2,3\}$.*
3. *The function S_A has no critical zero on the open side $[OB]$, and no critical zero on the open median $[AM_A]$.*

Remark. With the usual parametrization of the edges, the critical zeros Z_{i,S_A} are associated with the values u_{i,S_A} defined by

$$\begin{aligned} u_{i,S_A} &= \tfrac{4}{3} - u_{i,S}\,, \text{ for } i \in \{1,2,3\}\,, \\ u_{3+i,S_A} &= \tfrac{2}{3} - u_{i,S}\,, \text{ for } i \in \{1,2,3\}\,. \end{aligned} \tag{8.21}$$

8.6 The nodal sets of $C_{2,3}$ and $S_{2,3}$

Properties 8.10 *Nodal sets of $C_{2,3}$ and $S_{2,3}$.*

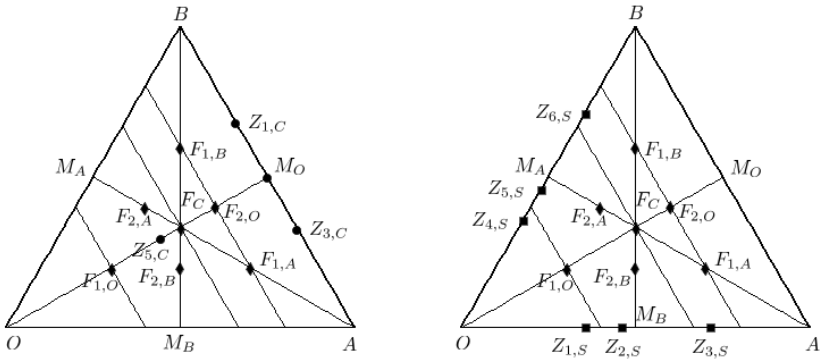

Figure 8.4: Barriers, fixed points and critical zeros for $N(C_{2,3})$ and $N(S_{2,3})$

1. *The function $C_{2,3}$ has only one critical zero $Z_{5,C}$ in the interior of the triangle $\mathcal{T}$. Its nodal set consists of the diagonal $[OM_O]$, and an injective regular arc from $Z_{1,C}$ to $Z_{3,C}$ which intersects $[OM_O]$ orthogonally at $Z_{5,C}$, and passes through the fixed points $F_{1,A}$, $F_{2,A}$, $F_{1,B}$ and $F_{2,B}$.*

2. *The function $S_{2,3}$ has no critical zero in the interior of the triangle. Its nodal set consists of three disjoint injective regular arcs: one from $Z_{1,S}$ to $Z_{4,S}$, passing through $F_{1,O}$; one from $Z_{2,S}$ to $Z_{5,S}$, passing through $F_{2,A}$, $F_{2,B}$, and F_C; one from $Z_{3,C}$ to $Z_{6,C}$, passing through $F_{1,A}$, $F_{2,O}$, and $F_{1,B}$.*

Proof. We already know that the nodal set $N(C_{2,3})$ contains the median $[OM_O]$. Except for this segment, no other nodal arc for either $C_{2,3}$ or $S_{2,3}$ can arrive at a vertex. Figure 8.4 displays the fixed points and the critical zeros for $N(C_{2,3})$ (left) and $N(S_{2,3})$ (right). We know the local behaviour of the nodal sets near the fixed points F_*, and near the critical zeros Z_*. The partial barriers (see Subsection 8.4) are also shown in Figure 8.4. The nodal sets $N(C_{2,3})$ and $N(S_{2,3})$ cannot meet the barriers except at one of the points F_* or Z_*.

The medians divide $\mathcal{T}$ into six isometric H-triangles. The nodal sets of $C_{2,3}$ and $S_{2,3}$ consist of finitely many nodal arcs which are smooth except at the critical zeros. They can only exit the interior of an H-triangle at a fixed point or at a critical zero.

Nodal set $N(C_{2,3})$. It suffices to look at the subset $N' := (N(C_{2,3}) \setminus [OM_O]) \cup \{Z_{5,C}\}$.

First of all, notice that for each H-triangle determined by the medians of $\mathcal{T}$, there are exactly two exit points for an arc belonging to N', with only one exit direction at each point. Indeed, except for the edges contained in the median $[OM]$, each edge contains at most one exit point (a fixed point or a critical zero). Furthermore, the vertices of the H-triangles are not exit points.

We claim that the function $C_{2,3}$ cannot have any critical zero in the interiors of the H-triangles. Indeed, assume that there is one critical zero $Z \in N'$ in the interior of some H-triangle $\mathcal{H}$. At this point, the nodal set would consist of at least four semi-

arcs. Following any such semi-arc, we either obtain a simply closed nodal arc, or exit the triangle. Since there are at most two exit points, there would be at least one simply closed nodal component in the interior of the triangle $\mathcal{H}$. This component would bound at least one nodal domain ω. The first Dirichlet eigenvalue $\lambda(\omega)$ would satisfy $\lambda(\omega) = \lambda_7(\mathcal{T}) = 19$. On the other-hand, since ω is contained in the interior of $\mathcal{H}$, we would have $\lambda(\omega) > \lambda(\mathcal{H}) = 21$ according to Lemma 7.3, a contradiction.

The last argument in the proof of the claim also shows that the interiors of the H-triangles cannot contain any closed nodal component of $C_{2,3}$. This shows that the nodal set of $C_{2,3}$ is indeed as shown in Figure 5.2.

Nodal set $N(S_{2,3})$. First of all, notice that for the H-triangle determined by the medians of $\mathcal{T}$, there are either two or four exit points, with only one exit direction at each point. More precisely, there are three cases.

Case (i). The triangles $T(F_C, B, M_O)$ and $T(F_C, A, M_O)$ have two exit points which are fixed points. The arguments used for $C_{2,3}$ apply for these triangles.

Case (ii). The triangles $T(F_C, O, M_A)$ and $T(F_C, O, M_B)$ have four exit points, two fixed points and two critical zeros on the open edges. We claim that the function $S_{2,3}$ cannot have any critical zero in the interiors of these H-triangles. Indeed, assume that there is one critical zero Z in the interior of such an H-triangle $\mathcal{H}$. At this point, the nodal set would consist of at least four semi-arcs. Following any such semi-arc, we either obtain a simply closed nodal arc, or exit the triangle. The preceding arguments show that we cannot have any simply closed nodal component inside $\mathcal{H}$. Since there are four exit points, each of them with a single exit direction, we would have two arcs joining the exit points and meeting at the critical zero Z. This would yield a nodal domain ω bounded by two semi-arcs and a segment in one of the edges of $\mathcal{T}$, or at least one simply closed nodal component in the interior of the triangle $\mathcal{H}$. The first Dirichlet eigenvalue $\lambda(\omega)$ would satisfy $\lambda(\omega) = \lambda_7(\mathcal{T}) = 19$. On the other-hand, since ω is contained in the interior of $\mathcal{H}$, we would have $\lambda(\omega) > \lambda(\mathcal{H}) = 21$, according to Lemma 7.3, a contradiction.

Case (iii). The triangles $T(F_C, B, M_A)$ and $T(F_C, A, M_B)$ have four exit points, the vertex F_C, two fixed points on the open edges, and one critical zero on an open edge. We begin with the same argument as in the previous case. To conclude, we use the barriers given by Lemma 8.3.

The above proofs also show that the interiors of the H-triangles cannot contain any closed nodal component of $S_{2,3}$. This shows that the nodal set of $S_{2,3}$ is indeed as shown in Figure 5.2. □

8.7 Critical zeros of $\Psi^\theta_{2,3}$ on the sides of $\mathcal{T}$, for $\theta \in]0, \frac{\pi}{6}]$

As a consequence of Properties 8.4, the critical zeros of the functions $\Psi^\theta_{2,3}$ on the sides of the triangle $\mathcal{T}$ are determined by one of the equations

$$\cos\theta\, FC(u) \pm \sin\theta\, FS(u) = 0\,.$$

Recall that for $\theta \in]0, \frac{\pi}{6}]$, the vertices of $\mathcal{T}$ are critical zeros of order 3 of $\Psi^\theta_{2,3}$ (Properties 8.1).

Properties 8.11 *The critical zeros of the function $\Psi^\theta_{2,3}$ on the open edges of the triangle $\mathcal{T}$ are determined by the following equations.*

1. *On the edge $[OA]$ parametrized by $u \mapsto (u, u/2)$,*

$$\cos\theta\, FC(u) + \sin\theta\, FS(u) = 0\,, \quad \text{for } u \in [0, 2/3]\,. \tag{8.22}$$

2. *On the edge $[OB]$ parametrized by $u \mapsto (u/2, u)$,*

$$\cos\theta\, FC(u) - \sin\theta\, FS(u) = 0\,, \quad \text{for } u \in [0, 2/3]\,. \tag{8.23}$$

3. *On the edge $[BA]$ parametrized by $u \mapsto (u/2, 1 - u/2)$,*

$$\cos\theta\, FC(u) - \sin\theta\, FS(u) = 0\,, \quad \text{for } u \in [2/3, 4/3]\,. \tag{8.24}$$

For convenience, we introduce the functions,

$$K^\theta_\pm(u) = \cos\theta\, FC(u) \pm \sin\theta\, FS(u)\,. \tag{8.25}$$

Properties 8.12 *Recall the notation* (8.20).

1. *Zeros of K^θ_+ in the interval $]0, 2/3[$ (corresponding to critical zeros on the open side $[OA]$). There exists $u_b \in]\frac{1}{3}, u_{3,S}[$, and $\theta_c \in]0, \frac{\pi}{6}[$ such that:*

   (a) *if $0 < \theta < \theta_c$, the function K^θ_+ has only one simple zero $\alpha_1(\theta) \in]0, u_{6,S_A}]$;*

   (b) *if $\theta = \theta_c$, the function K^θ_+ has a simple zero $\alpha_1(\theta_c) \in]0, u_{6,S_A}]$, and a double zero at u_b.*

   (c) *if $\theta_c < \theta \leq \frac{\pi}{6}$, the function K^θ_+ has three simple zeros, $\alpha_1(\theta) \in]0, u_{6,S_A}]$, $\alpha_2(\theta) \in [u_{5,S_A}, u_b[$, and $\alpha_3(\theta) \in]u_b, u_{4,S_A}]$.*

   The function $\alpha_1(\theta)$ and $\alpha_3(\theta)$ are increasing. The function $\alpha_2(\theta)$ is decreasing.

2. *Zeros of K^θ_- in the interval $]0, 2/3[$ (corresponding to critical zeros on the open side $[OB]$). In this interval, the function K^θ_- does not vanish.*

3. *Zeros of K^θ_- in the interval $]2/3, 4/3[$ (corresponding to critical zeros on the open side $[BA]$).The function H^θ_- has three simple zeros $\omega_1(\theta) \in [u_{3,S_A}, u_{1,C}[$, $\omega_2(\theta) \in]1, u_{2,S_A}]$, and $\omega_3(\theta) \in [u_{1,S_A}, u_{3,C}[$. The functions ω_1 and ω_3 are decreasing, the function ω_2 is increasing.*

Proof. Notice that the zeros are continuous with respect to θ (indeed, the equations can be transformed into polynomials whose coefficients are continuous in θ). An information on the possible location of zeros in given by Table 8.1, depending on the value of θ, see lines 7 and 9 in the table.

We first investigate whether the zeros of $K^{\theta}_{\pm}$ can have order at least 2. More precisely, we investigate whether there exists a pair (θ, u) such that

$$\begin{array}{l} \cos\theta\, FC(u) \pm \sin\theta\, FS(u) = 0\,, \\ \cos\theta\, FC'(u) \pm \sin\theta\, FS'(u) = 0\,. \end{array} \tag{8.26}$$

For this purpose, we define the function

$$WFCS(u) := FC(u)FS'(u) - FS(u)FC'(u). \tag{8.27}$$

Lemma 8.13 *Define the polynomial*

$$P_W(x) := -6x^5 + 25x^3 - 15x^2 - 15x + 11\,. \tag{8.28}$$

Then,

$$\begin{array}{rcl} \frac{1}{2\pi} WFCS(u) & = & 28 + 3\sin(8\pi u)\sin(7\pi u) - 3\cos(8\pi u)\cos(7\pi u) \\ & & \quad - 35\sin(8\pi u)\sin(\pi u) + 35\cos(8\pi u)\cos(\pi u) \\ & & \quad - 60\sin(7\pi u)\sin(\pi u) - 60\cos(7\pi u)\cos(\pi u) \\ & = & 28 - 3\cos(15\pi u) + 35\cos(9\pi u) - 60\cos(6\pi u) \\ & = & 8P_W\left(\cos(3\pi u)\right)\,. \end{array} \tag{8.29}$$

The polynomial P_W factors as

$$P_W(x) = -(x-1)^3(x+\xi)(x+\eta)\,, \tag{8.30}$$

where

$$\xi = \frac{9-\sqrt{15}}{6} \text{ and } \eta = \frac{9+\sqrt{15}}{6}\,. \tag{8.31}$$

Let

$$u_{0,W} := \frac{1}{3\pi}\arccos(\xi) \approx 0.2753793461\,. \tag{8.32}$$

In the interval $]-1/6, 3/2[$, the function $WFCS$ vanishes at the points $u \in \{0, \frac{2}{3}, \frac{4}{3}\}$ (which correspond to vertices), and at the points $\{u_{1,W}, u_{2,W}, u_{3,W}, u_{4,W}\}$, where

$$\begin{array}{lll} u_{1,W} & = \frac{1}{3} - u_{0,W} & \approx 0.2753793461\,, \\ u_{2,W} & = \frac{1}{3} + u_{0,W} & \approx 0.3912873205\,, \\ u_{3,W} & = 1 - u_{0,W} & \approx 0.9420460128\,, \\ u_{4,W} & = 1 + u_{0,W} & \approx 1.057953987\,. \end{array} \tag{8.33}$$

The points $u_{i,W}$, are simple zeros of the function $WFCS$.

Proof of the lemma.
Equations (8.29) follow by computing the derivatives of FC and FS, by expanding the expression of $WFCS$, and by making use of the Chebyshev polynomials. The remaining part of the lemma follows easily. □

Recall that $\theta \in]0, \frac{\pi}{6}]$. If $WFCS(u) \neq 0$, the system (8.26) has no solution (θ, u). If (θ, u) is a solution of the system (8.26), then $WFCS(u) = 0$, and $\cos\theta FC(u) \pm \sin\theta FS(u) = 0$,

which implies that $\pm\frac{FC(u)}{FS(u)} \in]0, \sqrt{3}]$. Computing this ratio for the above values $u_{i,W}$, we conclude that $u_{2,W}$ is the unique value for which the condition can be satisfied, and this only occurs for the function K^θ_+.

Define

$$\begin{aligned} u_b &:= u_{2,W} \approx 0.3912873205\,, \\ \theta_c &:= \arctan\left(\tfrac{FC(u_b)}{FS(u_b)}\right) \approx 0.3005211736\,. \end{aligned} \tag{8.34}$$

What we have just proved is that, for all $\theta \in]0, \frac{\pi}{6}]$, K^θ_- has only simple zeros in the set $]0, 2/3[\cup]2/3, 4/3[$; for all $\theta \in]0, \frac{\pi}{6}] \setminus \{\theta_c\}$, K^θ_+ has only simple zeros in the set $]0, 2/3[\cup]2/3, 4/3[$; for $\theta = \theta_c$, $K^{\theta_c}_+$ has exactly one double zero at u_b. This corresponds to a critical zero of order 3 on the edge $[OA]$.

Lemma 8.13 implies that for $\theta \in]0, \pi/6] \setminus \{\theta_c\}$, the zeros (if any) of the functions $K^\theta_\pm$ in the interval $]0, \frac{2}{3}[$ and $]\frac{2}{3}, \frac{4}{3}[$ are simple, so that they are smooth in θ. If $u(\theta)$ is such a zero, its derivative with respect to θ satisfies the relation

$$1 + \tan^2(\theta) = \pm \frac{WCS(u(\theta))}{GS^2(u(\theta))} u'(\theta)\,.$$

We can now start from the function $\Psi^{\frac{\pi}{6}}_{2,3} = -S_B$, and follow the zeros by continuity, using Corollary 8.9. This proves Properties 8.12 on the open edge $[OA]$ when $\theta_c < \theta < \frac{\pi}{6}$, and on the open edges $[OB]$ and $[BA]$ for all θ. When $\theta = \theta_c$, we have a critical zero of order 2 and a critical zero of order 3 on $[OA]$. It is easy to see that for $\theta > 0$ very small, there is only one critical zero on the open edge $[OA]$, and we can follow this zero by continuity for $0 < \theta < \theta_c$. □

$u \in [0, 4/3]$	$\approx$	GC	GS	H^θ_+	H^θ_-
0	0	0	≈ 3.7500	$\approx 3.7500 \sin\theta$	$\approx -3.7500 \sin\theta$
$\alpha_1(\theta)$	–	–	–	0	–
$u_{1,S}$	≈ 0.2413	≈ -0.4167	≈ 0	$\approx -0.4167 \cos\theta$	$\approx -0.4167 \cos\theta$
$u_{2,S}$	≈ 0.3085	≈ -0.2959	≈ 0	$\approx -0.2959 \cos\theta$	$\approx -0.2959 \cos\theta$
$\frac{1}{3}$	≈ 0.3333	≈ -0.2165	≈ 0.1250	$\approx -0.2165 \cos\theta + 0.1250 \sin\theta$	$\approx -0.2165 \cos\theta - 0.1250 \sin\theta$
$\alpha_2(\theta)$	–	–	–	0 (if $\theta \geq \theta_c$)	–
u_{bif}	≈ 0.3913	≈ -0.1161	≈ 0.3745	$\approx -0.1161 \cos\theta + 0.3745 \sin\theta$	$\approx -0.1161 \cos\theta - 0.3745 \sin\theta$
$\alpha_3(\theta)$	–	–	–	0 (if $\theta \geq \theta_c$)	–
$u_{3,S}$	≈ 0.4784	$\approx -.6885$	≈ 0	$\approx -0.6885 \cos\theta$	$\approx -0.6885 \cos\theta$
$\frac{2}{3}$	≈ 0.6667	≈ -3.2476	≈ -1.8750	$\approx -3.2476 \cos\theta - 1.8750 \sin\theta$	$\approx -3.2476 \cos\theta + 1.8750 \sin\theta$
$u_{3,SB}$	≈ 0.8549	≈ -0.3442	≈ -0.5962	$\approx -0.3442 \cos\theta - 0.5962 \sin\theta$	$\approx -0.3442 \cos\theta + 0.5962 \sin\theta$
$\omega_1(\theta)$	–	–	–	–	0
$u_{1,C}$	≈ 0.8812	≈ 0	$\approx -.4588$	$\approx -0.4588 \sin\theta$	$\approx 0.4588 \sin\theta$
$u_{2,C}$	1	≈ 0	$\approx -.2500$	$\approx -0.2500 \sin\theta$	$\approx 0.2500 \sin\theta$
$\omega_2(\theta)$	–	–	–	–	0
$u_{2,SB}$	≈ 1.02480	≈ -0.1479	≈ -0.2562	$\approx -0.1479 \cos\theta - 0.2562 \sin\theta$	$\approx -0.1479 \cos\theta + 0.2562 \sin\theta$
$u_{1,SB}$	≈ 1.0920	≈ -0.2083	≈ -0.3609	$\approx -0.2083 \cos\theta - 0.3609 \sin\theta$	$\approx -0.2083 \cos\theta + 0.3609 \sin\theta$
$\omega_3(\theta)$	–	–	–	–	0
$u_{3,C}$	≈ 1.1188	≈ 0	≈ -0.4588	$\approx -0.4588 \sin\theta$	$\approx 0.4588 \sin\theta$
$\frac{4}{3}$	≈ 1.3333	≈ 3.2476	≈ -1.8750	$\approx 3.2476 \cos\theta - 1.8750 \sin\theta$	$\approx 3.2476 \cos\theta + 1.8750 \sin\theta$

Table 8.1: Values of $K^\theta_\pm$

Corollary 8.14 *Critical zeros of the function* $\Psi^{\theta}_{2,3}$ *for* $\theta \in]0, \frac{\pi}{6}]$.

1. *The function* $\Psi^{\theta}_{2,3}$ *always has one critical zero of order* 2 $Z_{6,\theta} \in]O, Z_{6,S_A}]$.
   - *If* $\theta < \theta_c$ *, the function* $\Psi^{\theta}_{2,3}$ *has no other critical zero on the open edge* $[OA]$.
   - *If* $\theta = \theta_c$ *, the function* $\Psi^{\theta}_{2,3}$ *has also a critical zero* Z_b *of order* 3 *in the interval* $]Z_{5,S_A}, Z_{6,S_A}[$.
   - *If* $\theta > \theta_c$ *, the function* $\Psi^{\theta}_{2,3}$ *has also two critical zeros of order* 2, $Z_{5,\theta} \in [Z_{5,S_A}, Z_b[$ *and* $Z_{4,\theta} \in]Z_b, Z_{4,\theta}]$ *.*
2. *The function* $\Psi^{\theta}_{2,3}$ *has three critical zeros of order* 2 *on the open edge* $[BA]$*:* $Z_{3,\theta} \in [Z_{3,S_A}, Z_{1,C}[$ *,* $Z_{2,\theta} \in]Z_{2,C}, Z_{2,S_A}]$ *, and* $Z_{1,\theta} \in [Z_{1,S_A}, Z_{3,C}[$ *.*
3. *The function* $\Psi^{\theta}_{2,3}$ *has no critical zero on the open edge* $[OB]$.

The corollary is illustrated by Figure 8.5: the picture on the left shows the fixed points, the boundary critical zeros of $C_{2,3}$ and S_A, as well as the nodal sets $N(C_{2,3})$ and $N(S_A)$ (Maple calculation). The picture on the right shows the fixed points and the boundary critical zeros for $\Psi^{\theta}_{2,3}$.

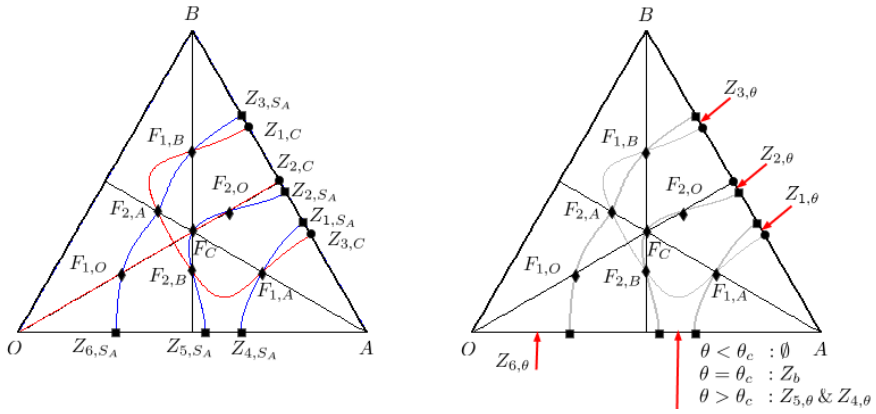

Figure 8.5: Boundary critical zeros for C, S_A , and $\Psi^{\theta}_{2,3}$

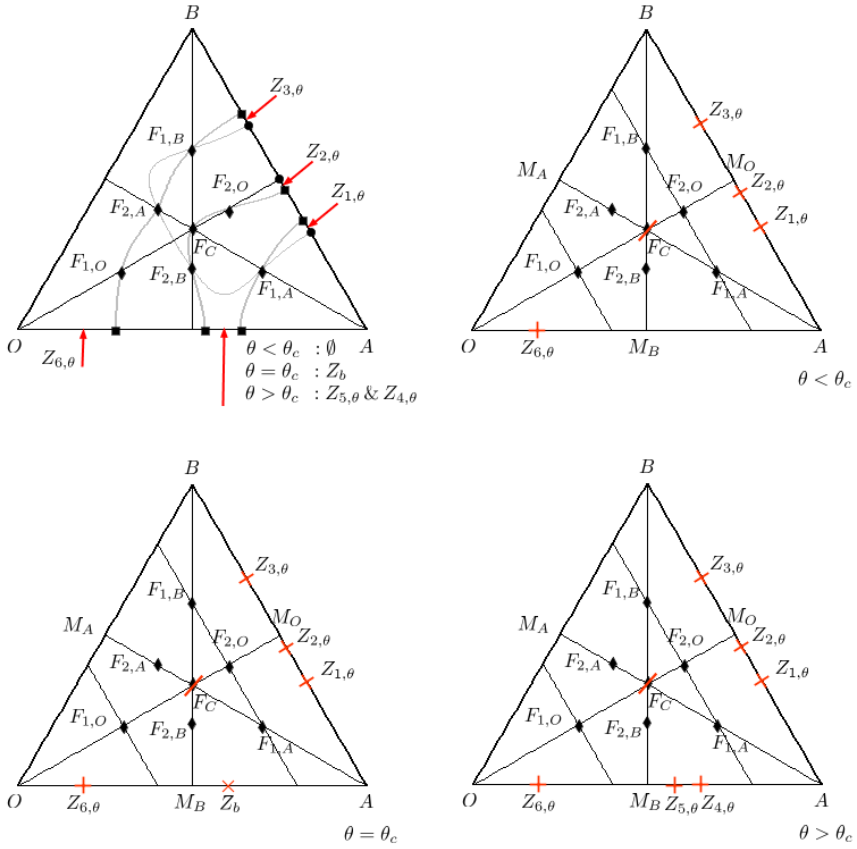

Figure 8.6: Boundary critical zeros for $\Psi^{\theta}_{2,3}$

8.8 Nodal set of $\Psi^{\theta}_{2,3}$

Proposition 8.15

1. *For $\theta \in]0, \theta_c[$ the nodal set of $\Psi^{\theta}_{2,3}$ consists of two disjoint injective arcs, one from $Z_{6,\theta}$ to $Z_{3,\theta}$, through $F_{1,O}$, $F_{2,A}$, and $F_{1,B}$, another from $Z_{1,\theta}$ to $Z_{2,\theta,}$, through the points $\{F_{1,A}$, $F_{2,B}$, F_C and $F_{2,O}\}$. In particular, the function $\Psi^{\theta}_{2,3}$ has three nodal domains.*

2. *For $\theta = \theta_c$, the nodal set of $\Psi^{\theta}_{2,3}$ consists of three disjoint injective arcs, one from $Z_{6,\theta}$ to $Z_{3,\theta}$ through the points $F_{1,O}$ $F_{2,A}$, and $F_{1,B}$; one from Z_b to $Z_{2,\theta}$, through the points $F_{2,B}$, F_C, and $F_{2,O}$; one from Z_b to $Z_{1,\theta}$, through the point $F_{1,A}$. In particular, the eigenfunction has four nodal domains.*

3. *For $\theta_c < \theta \leq \frac{\pi}{6}$, the nodal set of $\Psi^{\theta}_{2,3}$ consists of three disjoint injective arcs, one from $Z_{6,\theta}$ to $Z_{3,\theta}$ through the points $F_{1,O}$ $F_{2,A}$, and $F_{1,B}$; one from $Z_{5,\theta}$ to $Z_{2,\theta}$, through the points $F_{2,B}$, F_C, and $F_{2,O}$; one from $Z_{4,\theta}$ to $Z_{1,\theta}$, through the point $F_{1,A}$. In particular, the eigenfunction has four nodal domains.*

As a consequence, the eigenvalue $\lambda_7(\mathcal{T}) = 17$ is not Courant-sharp.

Proof. We determine the nodal set of $\Psi^\theta_{2,3}$ in each of the six H-triangles determined by the medians of the triangle $\mathcal{T}$.

We first observe that the nodal set has a tangent at the point F_C which makes an angle less than $\frac{\pi}{6}$ with $[OM]$. This implies that the point F_C is an exit point for two H-triangles only, namely $T(B, F_C, M_O)$ and $T(O, F_C, M_B)$.

For $a \in [0, 1]$, we consider the functions

$$BP^\theta_a(u) = \Psi^\theta_{2,3}(u, a-u)\,, \tag{8.35}$$

for $u \in [\frac{a}{3}, \frac{2a}{3}]$ i.e., the restrictions of the functions $\Psi^\theta_{2,3}$ to the segments $[B_aA_a] = D_a \cap \mathcal{T}$, whose end points B_a and A_a correspond to the values $\frac{a}{3}$ and $\frac{2a}{3}$ of u. We call M_a the mid-point of this segment i.e., its intersection with the median $[OM]$. More precisely, we consider the functions $BP_{\frac{2}{5}}$ and $BP_{\frac{4}{5}}$. According to the proof of Lemma 8.3, we have the formulas

$$\begin{aligned} BP_{\frac{2}{5}} &= -4\sin(\tfrac{\pi}{5})\sin(15\pi u)\sin(\pi u + \tfrac{3\pi}{10} - \theta) \text{ for } u \in [\tfrac{2}{15}, \tfrac{4}{15}]\,, \\ BP_{\frac{4}{5}} &= -4\sin(\tfrac{\pi}{10})\sin(15\pi u)\sin(\pi u + \tfrac{\pi}{10} - \theta) \text{ for } u \in [\tfrac{4}{15}, \tfrac{8}{15}]\,. \end{aligned} \tag{8.36}$$

Taking into account the intervals for u, and the fact that $0 < \theta \leq \frac{\pi}{6}$, we can conclude that the corresponding segments are barriers inside the H-triangles which they intersect.

Figure 8.6 shows the three possible configurations depending on the number of critical zeros of the function $\Psi^\theta_{2,3}$ on the open edge $[OA]$.

The nodal set $N(\Psi^\theta_{2,3})$ consists of finitely many regular arcs which can only cross at critical zeros (including at the boundary). Because $\theta \in]0, \frac{\pi}{6}]$, no nodal arc arrives at a vertex. Because the fixed points are regular points, there is only one nodal arc at each fixed points. Only one nodal arc arrives at a boundary critical zero of order 2 (all of them except Z_b). Exactly two nodal arcs arrive at Z_b, with equal angles.

We work in each H-triangle separately. When working in a given H-triangle $\mathcal{H}$, we call *exit point* a point at which a nodal arc can exit the triangle. Because medians are partial barriers (Lemma 8.2), an exit point is either a fixed point, or a boundary critical zero.

Assume that Z is a critical zero of $\Psi^\theta_{2,3}$, in the interior of some H-triangle $\mathcal{H}$. There are at least four semi-arcs emanating from Z, and we can follow each one of them. Following such an arc, there are only two possibilities: either we arrive at an exit point, or the path we follow is not injective. The latter necessarily occurs if there are at most three exit directions. However, if a nodal path is not injective, it bounds at least a nodal domain $\omega \subset \mathcal{H}$, and hence its first Dirichlet eigenvalue satisfies $\lambda(\omega) = \lambda_7 = 19$. On the other-hand, $\lambda(\omega) > \lambda(\mathcal{H}) = 21$ (Lemma 7.3). More generally, we have proved the following property.

Lemma 8.16 *Assume $\mathcal{D} \subset \mathcal{H}$ is bounded by partial barriers, with at most 3 exit directions. Then $\mathcal{D}$ cannot contain any critical zero in its interior.*

We now make a case by case analysis of the six H-triangles contained in $\mathcal{T}$, for the notation, see Figure 8.6.

• Triangle $T(B, F_C, M_A)$. There are two exit points $F_{1,B}$ and $F_{2,A}$, each one with one exit direction. Note that F_C is not an exit point. We can apply Lemma 8.16, and conclude that the nodal set $N(\Psi^\theta_{2,3})$ inside this H-triangle is an arc from $F_{1,B}$ to $F_{2,A}$, without self-intersections.

• Triangle $T(O, F_C, M_A)$. Same arguments as in the preceding case, the nodal set inside this H-triangle is an arc from $F_{2,A}$ to $F_{1,O}$, without self-intersections.

• Triangle $T(O, F_C, M_B)$. In this H-triangle, there are 4 exit points, with one direction each: F_C, $F_{1,O}$, $F_{2,B}$, and $Z_{6,\theta}$. The barrier $D_{\frac{2}{5}}$ meets $N(\Psi^\theta_{2,3})$ at only one point, $F_{1,O}$. In particular, this segment cannot contain any critical zero and divided the H-triangle into two sub-domains with two exit points. We can apply Lemma 8.16 to each sub-domain, and conclude that the nodal set inside the H-triangle consists of two disjoint arcs without self-intersections, one from $F_{1,O}$ to $Z_{6,\theta}$, and one from F_C to $F_{2,B}$.

• Triangle $T(A, F_C, M_B)$. For this H-triangle, we have to consider three cases depending on the sign of $\theta - \theta_c$.

(i) Assume $0 < \theta < \theta_c$. In this case, there are only two exit points in this H-triangle, and we can reason as in the case of the triangle $T(B, F_C, M_A)$, concluding that the nodal set inside $T(A, F_C, M_B)$ is an arc from $F_{2,B}$ to $F_{1,A}$, without self-intersections.

(ii) Assume $\theta = \theta_c$. In this case, we have three exist points and 4 exit directions because Z_b is of order 3. Using the arguments as in the proof of Lemma 8.16, the existence of an interior critical zero would either yield an interior nodal loop, or a nodal loop touching the boundary at Z_b. In either case, the energy argument works, and we can conclude that the nodal set inside $T(A, F_C, M_B)$ consists of two disjoint arcs without self-intersections, one from Z_b to $F_{2,B}$, and one from Z_b to $F_{1,A}$.

(iii) Assume $\theta > \theta_c$. Similar to the preceding case, assuming there is an interior critical zero Z, we would either get an interior nodal loop, or a curve from $Z_{4,\theta}$ to Z, to $Z_{5,\theta}$. We would then get a nodal domain contained in $T(A, F_C, M_B)$ and with boundary intersecting the edge $[OA]$. The energy argument applies, and we can conclude that the nodal set consists of two disjoint curves without self-intersections, one from $Z_{5,\theta}$ to $F_{2,3}$, and one from $Z_{4,\theta}$ to $F_{1,A}$.

• Triangle $T(A, F_C, M_O)$. There are 4 exit points, with one direction each. Same treatment as for Triangle $T(A, F_C, M_B)$.

• Triangle $T(B, F_C, M_O)$. There are 4 exit points, with one exit direction each. Using the barrier $D_{\frac{4}{5}}$, this triangle can be divided into two sub-domains, each with 3 exit points. It follows that there are no interior critical zero in this H-triangle. It follows that the nodal set consists of two disjoint arcs without self-intersections joining pairs of exit points. This excludes (as the barrier $D_{\frac{4}{5}}$ does) the possibility of two arcs $(F_C, Z_{3,\theta})$ and $(F_{2,O}, F_{1,B})$. We are left with two possibilities,

(i) an arc $(F_C, F_{1,B})$ and an arc $(Z_{3,\theta}, F_{2,O})$, or

(ii) an arc $(F_C, F_{2,O})$ and an arc $(F_{1,B}, Z_{3,\theta})$.

For continuity reasons, (ii) holds for θ small enough. In both cases, the number of nodal domains is at most 4, and we can conclude that the eigenvalue λ_7 is not Courant-sharp.

In fact both case (i) and (ii) yield at most 4 nodal domains. □

Remarks.
(i) Let Ψ be an eigenfunction. Once one knows the critical zeros of Ψ, together with their orders, and the number of connected components of $N(\Psi) \cap \partial\mathcal{T}$, one can apply the Euler-type formula of [10, Proposition 2.8] to obtain the number of nodal domains of Ψ. Using the proof of Proposition 8.15 and this formula, one can recover the number of nodal domains of $\Psi^\theta_{1,3}$: three for $\theta \in]0, \theta_c[$, and four for $\theta \in [\theta_c, \frac{\pi}{6}]$.

(ii) It turns out that case (i) at the end of the previous proof can be discarded by yet another barrier. Indeed, we can consider the segment determined in $\mathcal{T}$ by the line through $F_{1,O}$ and parallel to $[OA]$, whose equation in the parametrization $\mathcal{F}$ is $s - 2t + \frac{3}{5} = 0$. It is parametrized by

$$u \mapsto \left(2u - \frac{3}{5}, u\right) \text{ for } u \in [\frac{2}{5}, \frac{8}{15}]\,. \tag{8.37}$$

As in the proof of Lemma 8.3, we define the functions

$$\begin{aligned} EC(u) &:= C_{2,3}(2u - \tfrac{3}{5}, u)\,, \\ ES(u) &:= S_{2,3}(2u - \tfrac{3}{5}, u)\,, \\ EP^\theta(u) &:= \Psi^\theta_{2,3}(2u - \tfrac{3}{5}, u)\,, \end{aligned} \tag{8.38}$$

and we obtain the relations,

$$\begin{aligned} EC(u) &= 4\sin(\tfrac{\pi}{5})\sin(15\pi u)\cos(\pi u + \tfrac{\pi}{5})\,, \\ ES(u) &= -4\sin(\tfrac{\pi}{5})\sin(15\pi u)\sin(\pi u + \tfrac{\pi}{5})\,, \\ EP^\theta(u) &= -4\sin(\tfrac{\pi}{5})\sin(15\pi u)\cos(\pi u + \tfrac{\pi}{5} + \theta)\,. \end{aligned} \tag{8.39}$$

Figure 8.7 shows a Maple simulation with the two bifurcations which occur in the interval $[0, \frac{\pi}{6}]$, namely at 0 (the inner critical zero disappears) and at θ_c, with a critical zero of order 3 on the edge $[OA]$.

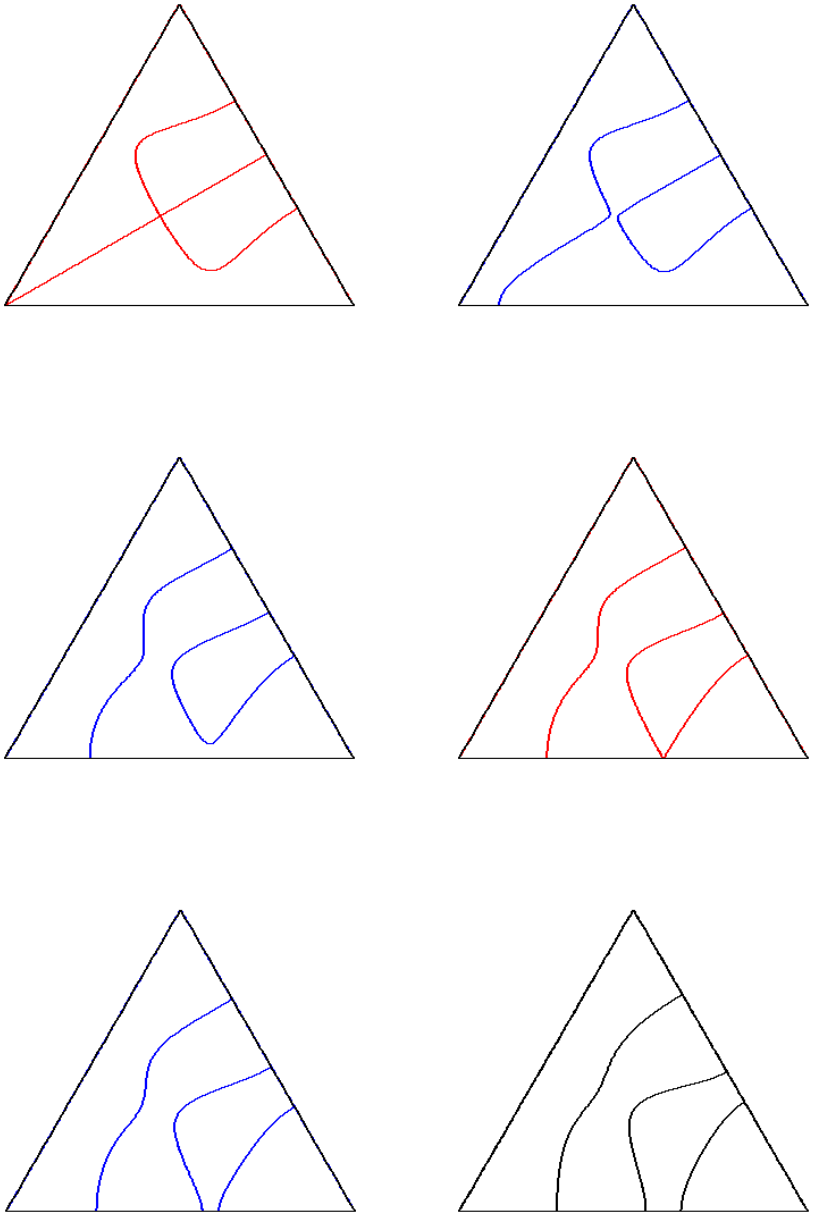

Figure 8.7: Bifurcations for $N(\Psi^{\theta}_{2,3}), \theta \in]0, \frac{\pi}{12}]$

9 Equilateral triangle: epilogue

Provided one can give a full description of the nodal sets $N(C_{m,n})$ and $N(S_{m,n})$, for $(m,n) = (1,3)$ or $(2,3)$, one can use the checkerboard argument associated with the pair $(C_{m,n}, S_{m,n})$ mentioned in Section 6. Since we work with $\theta \in [0, \frac{\pi}{6}]$, it is actually more

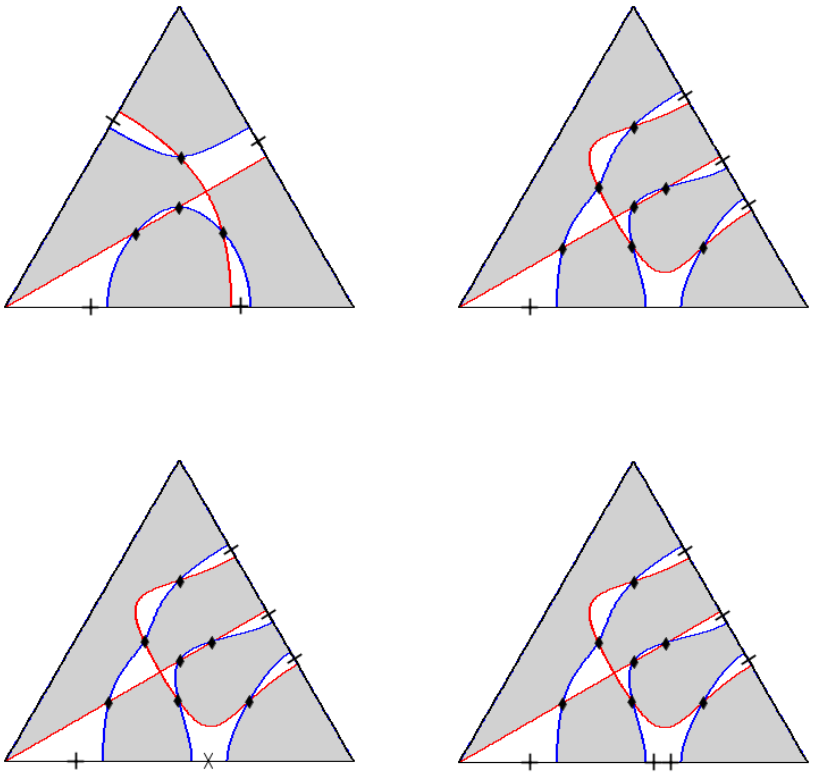

Figure 9.1: Adapted checkerboards

appropriate to work with the checkerboard associated with the pair $(C_{m,n}, \Psi^{\frac{\pi}{6}}_{m,n})$. Indeed,

$$\sin(\frac{\pi}{6})\Psi^{\theta}_{m,n} = \sin(\frac{\pi}{6} - \theta)C_{m,n} + \sin(\theta)\Psi^{\frac{\pi}{6}}_{m,n}\,.$$

We have the inclusion

$$N(\Psi^{\theta}_{m,n}) \subset \{C_{m,n}\,\Psi^{\frac{\pi}{6}}_{m,n} < 0\} \cup (N(C_{m,n}) \cap N(S_{m,n}))\,.$$

Figure 9.1 displays this checkerboard in the case $(m, n) = (1, 3)$ (top row, left), and in the three sub-cases of the case $(m, n) = (2, 3)$, depending on the number of critical zeros on the edge $[OA]$ (top row right and bottom row). It is easy to see that the knowledge of the checkerboard and of the critical zeros on the edges determines the nodal set of $\Psi^{\theta}_{m,n}$ when $\theta \in]0, \frac{\pi}{6}]$. Indeed, recall that the rule is that a nodal line can only leave or enter a white component through points which belong to $N(C_{m,n}) \cap N(S_{m,n})$. But each white component has at most two points of this type in its closure. Note that this was not the case in the checkerboard presented in Figure 6.1, where we need to prove the existence of additional barriers to determine the nodal picture.

10 Other triangles

The rectangle, the equilateral triangle, the right-angled isosceles triangle, and the hemi-equilateral triangle, are the alcoves of the 2-dimensional root systems $A_1 \times A_1$, A_2, B_2 and G_2 respectively, [6]. Their Dirichlet and Neumann spectral data can be described completely, [2]. They are also the only plane polygonal domains all of whose Dirichlet or Neumann eigenfunctions are trigonometric [15, Chapt. IV].

The Dirichlet spectral data of the right-angled isosceles triangle and of the hemiequilateral triangle are easily deduced from the data for the square and of the equilateral triangle respectively. The investigation of the Courant-sharp Dirichlet eigenvalues of these triangles can also be done, using the above methods. It turns out to be simpler than the investigation of the Courant-sharp eigenvalues of the equilateral triangle. We sketch the proofs in the following sub-sections.

10.1 The right-angled isosceles triangle

Call $\mathcal{S}_\pi$ the open square with side π. A complete set of Dirichlet eigenfunctions is given by

$$\psi_{m,n}(x,y) = \sin(mx)\sin(ny)\,, \tag{10.1}$$

with associated eigenvalues m^2+n^2, where m and n are positive integers.

Call $\mathcal{B}_\pi$ the right-angled isosceles triangle,

$$\mathcal{B}_\pi = \left\{(x,y) \in]0,\pi[^2 \mid y < x\right\}\,. \tag{10.2}$$

A complete set of Dirichlet eigenfunctions for $\mathcal{B}_\pi$ is given by

$$\varphi_{m,n}(x,y) = \sin(mx)\sin(ny) - \sin(nx)\sin(my)\,, \tag{10.3}$$

with associated eigenvalues m^2+n^2, for positive integers m and n satisfying $1 \le n \le m-1$.

Denote by $N_{\mathcal{S}}(\lambda) = \#\{n \mid \lambda_n(\mathcal{S}_\pi) < \lambda\}$ the counting function of the Dirichlet eigenvalues of $\mathcal{S}_\pi$. Similarly denote by $N_{\mathcal{B}}(\lambda)$ the counting function of the Dirichlet eigenvalues of $\mathcal{B}_\pi$. Clearly,

$$N_{\mathcal{S}}(\lambda) = 2N_{\mathcal{B}}(\lambda) + \#\{m \in \mathbb{N}^\bullet \mid 2m^2 < \lambda\}\,. \tag{10.4}$$

Using [5, Equation (2.1)], we get the lower bound

$$N_{\mathcal{B}}(\lambda) \ge \frac{\pi\lambda}{8} - \frac{(4+\sqrt{2})\sqrt{\lambda}}{4} - \frac{1}{2}\,. \tag{10.5}$$

Using the Faber-Krahn inequality, a Courant-sharp eigenvalue $\lambda_n(\mathcal{B}_\pi)$ satisfies

$$\frac{\lambda_n(\mathcal{B}_\pi)}{n} \ge \frac{2}{\pi} j_{0,1}^2 \sim 3.681690532\,. \tag{10.6}$$

On the other-hand, if $\lambda_n(\mathcal{B}_\pi)$ is Courant-sharp, then $N_{\mathcal{B}}(\lambda_n(\mathcal{B}_\pi)) = n-1$. Using (10.5) and (10.6), we obtain the inequality

$$\frac{2}{\pi} j_{0,1}^2\, n \leq \left(\frac{4+\sqrt{2}}{\pi}\right)^2 \left(1+\sqrt{1+\frac{8\pi(n-\frac{1}{2})}{(4+\sqrt{2})^2}}\right)^2 . \tag{10.7}$$

Equation (10.7) shows that if $\lambda_n(\mathcal{B}_\pi)$ is Courant-sharp, then $n \leq 31$. Calculating the ratios $\frac{\lambda_n(\mathcal{B}_\pi)}{n}$ and using (10.6), we see that the only possible Courant-sharp Dirichlet eigenvalues of $\mathcal{B}_\pi$ are the $\lambda_n(\mathcal{B}_\pi)$ for $n \in \{1,\dots,7,9,10\}$. These eigenvalues have multiplicity 1, and correspond to the pairs

$$\{[2,1],[3,1],[3,2],[4,1],[4,2],[4,3],[5,1],[5,3],[6,1]\} . \tag{10.8}$$

To conclude, we have to determine the number $\mu(\varphi_{m,n})$ of nodal domains of the corresponding eigenfunctions $\varphi_{m,n}$.

Remark. The eigenvalues λ_5, λ_7 and λ_9 correspond to the pairs $[4,2],[5,1]$ and $[5,3]$ respectively. The associated eigenfunctions are anti-symmetric with respect to the line $\{x+y=\pi\}$. It follows that they have an even number of nodal domains. These eigenvalues cannot be Courant-sharp.

To deal with the other eigenvalues we use the following result [1], and the description of some nodal sets of Dirichlet eigenfunctions for the square membrane [5].

Properties 10.1 *The Dirichlet eigenfunctions $\varphi_{m,n}$ of the triangle $\mathcal{B}_\pi$ satisfy the following identities.*

1. *For $m > n$,*
$$\varphi_{m+n,m-n}(x,y) = \varphi_{m,n}(x+y, x-y) .$$
2. *If d is the greatest common divisor of m and n, then*
$$\varphi_{m,n}(x,y) = \varphi_{\frac{m}{d},\frac{n}{d}}(dx, dy) .$$

We obtain the following nodal count.

$\lambda_i(\mathcal{B}_\pi$	$[m,n]$	$\mu(\varphi_{m,n})$	using
λ_1	$[2,1]$	1	
λ_2	$[3,1]$	2	
λ_3	$[3,2]$	2	
λ_4	$[4,1]$	2	
λ_5	$[4,2]$	4	$\varphi_{2,1}$
λ_6	$[4,3]$	3	$\varphi_{7,1}$
λ_7	$[5,1]$	4	
λ_9	$[5,3]$	4	$\varphi_{8,2}, \varphi_{4,1}$
λ_{10}	$[6,1]$	3	

(10.9)

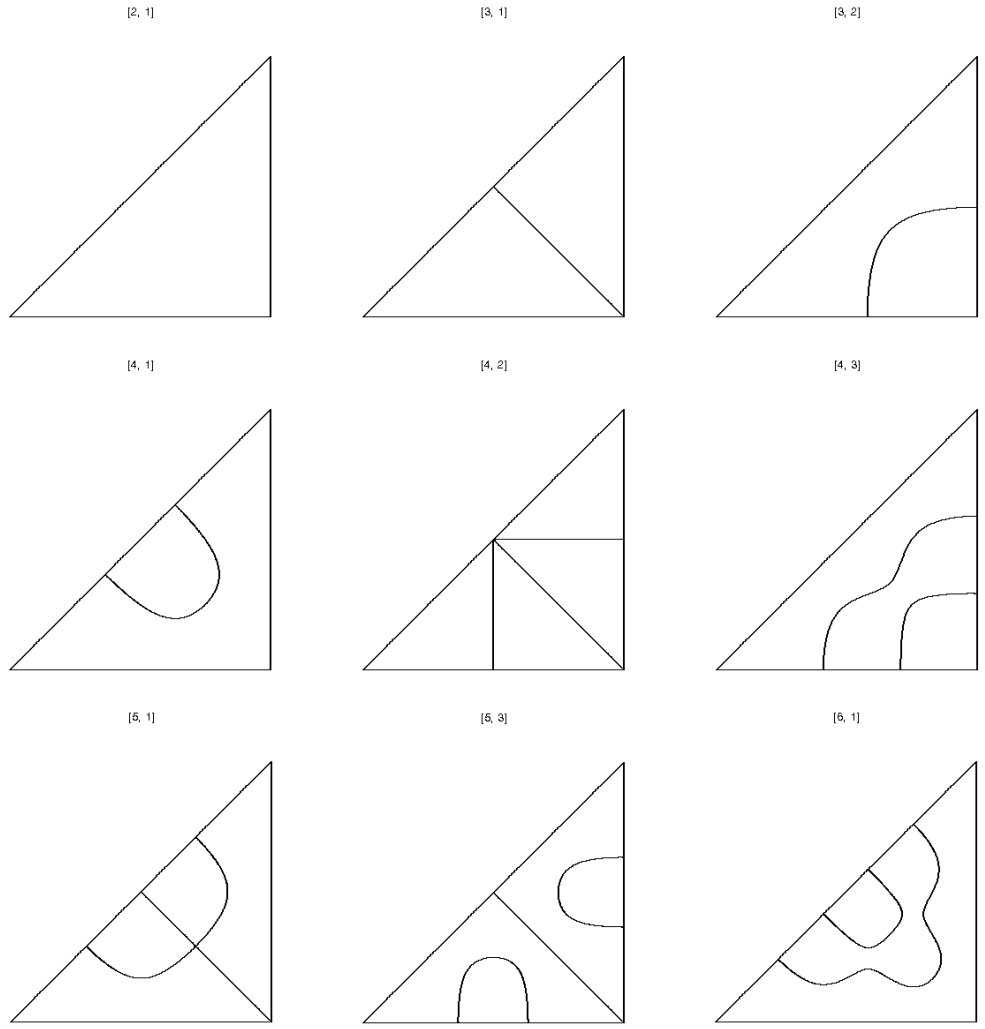

Figure 10.1: Courant-sharp analysis for the right-angled isosceles triangle

Theorem 10.2 *The only Courant-sharp eigenvalues of the right-angled triangle* $\mathcal{B}_\pi$ *are* $\lambda_1(\mathcal{B}_\pi)$ *and* $\lambda_2(\mathcal{B}_\pi)$.

Remark. A general algorithm to compute the number of nodal domains of the eigenfunctions $\varphi_{m,n}$ of the triangle $\mathcal{B}_\pi$ is described in [1].

10.2 The hemiequilateral triangle

A complete set of Dirichlet eigenfunctions of the hemiequilateral triangle $\mathcal{H}$, with hypothenuse of length 1, is given by the functions $C_{m,n}$ described in (4.8), with $1 \leq n < m$. The associated eigenvalues are the numbers $\frac{16\pi^2}{9}(m^2 + mn + n^2)$.

Using the Faber-Krahn inequality, we obtain that a Courant-sharp eigenvalue $\lambda_n(\mathcal{H})$

satisfies the inequality

$$\lambda_n(\mathcal{H}) \geq \frac{8\pi}{\sqrt{3}} j_{0,1}^2\, n. \tag{10.10}$$

The lower bound (5.2) yields the following lower bound for the counting function of the Dirichlet eigenvalues of $\mathcal{H}$,

$$N_{\mathcal{H}}(\lambda) \geq \frac{\sqrt{3}}{32\pi}\lambda - \frac{6+\sqrt{3}}{8\pi}\sqrt{\lambda} + \frac{1}{2}\,. \tag{10.11}$$

Using (10.10) and (10.11), we conclude that if $\lambda_n(\mathcal{H})$ is Courant-sharp, then $n \leq 32$. Using (10.10) again, we see that the only possible Courant-sharp eigenvalues are $\lambda_i(\mathcal{H})$, for $i \in \{1, \dots, 8, 10\}$. All these eigenvalues have multiplicity 1, and correspond to the pairs

$$\{[2,1],[3,1],[3,2],[4,1],[4,2],[5,1],[4,3],[5,2],[5,3]\}\ .$$

Since the eigenfunctions are given explicitly, we can numerically determine the nodal sets, and conclude.

Theorem 10.3 *The only Courant-sharp Dirichlet eigenvalues of the hemiequilateral triangle $\mathcal{H}$ are the first and second.*

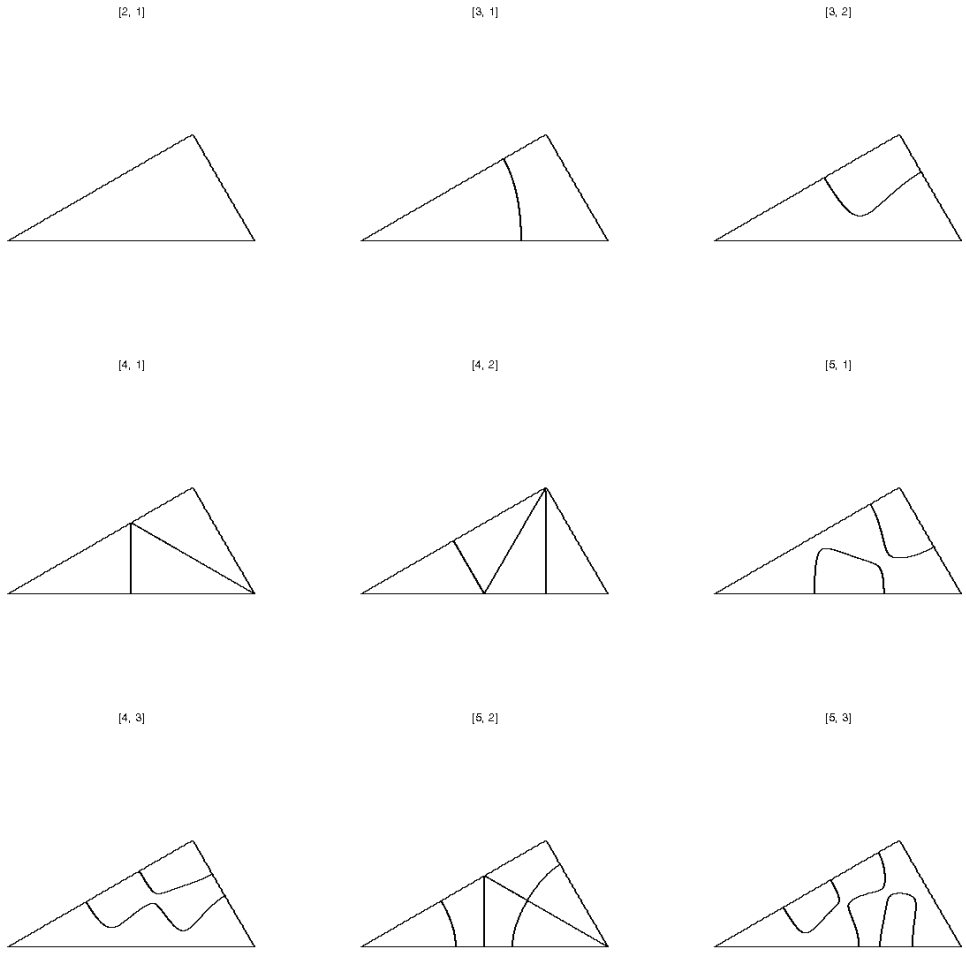

Figure 10.2: Courant-sharp analysis for the hemiequilateral triangle

References

[1] A. Aronovitch, R. Band, D. Fajman, and S. Gnutzmann. Nodal domains of a non-separable domain – the right-angled isosceles triangle. J. of Physics A **45** (2012) 085209.

[2] P. Bérard. Spectres et groupes cristallographiques I: Domaines euclidiens. Inventiones Math. **58** (1980), 179-199.

[3] P. Bérard and G. Besson. Spectres et groupes cristallographiques II: domaines sphériques. Ann. Inst. Fourier, Grenoble **3** (1980), 237-248.

[4] P. Bérard and B. Helffer. Remarks on the boundary set of spectral equipartitions. Phil. Trans. R. Soc. A 372:20120492.

[5] P. Bérard and B. Helffer. Dirichlet eigenfunctions of the square membrane: Courant's property, and A. Stern's and Å. Pleijel's analyses. arXiv:14026054. To appear in

Springer Proceedings in Mathematics & Statistics (2015), MIMS-GGTM conference in memory of M. S. Baouendi. Ali Baklouti, Aziz El Kacimi, Sadok Kallel, and Nordine Mir Editors.

[6] N. Bourbaki. Groupes et algèbres de Lie, Chapitres 4, 5 et 6. Hermann 1968.

[7] R. Courant. Ein allgemeiner Satz zur Theorie der Eigenfunktionen selbstadjungierter Differentialausdrücke. Nachr. Ges. Göttingen (1923), 81-84.

[8] Rayleigh-Faber-Krahn inequality. Encyclopedia of Mathematics. `http://www.encyclopediaofmath.org/index.php?title=Rayleigh-Faber-Krahn_inequality`

[9] B. Helffer and M. Persson-Sundqvist. Nodal domains in the square–the Neumann case. arXiv:1410.6702. To appear in Moscow Mathematical Journal.

[10] T. Hoffmann-Ostenhof, P.W. Michor, and N. Narirashvili. Bounds on the multiplicity of eigenvalues for fixed membranes. GAFA Geom. funct. anal. **9** (1999), 1169-1188.

[11] H. Howards, M. Hutchings, and F. Morgan. The isoperimetric problem on surfaces. Amer. Math. Monthly **106** (1999), 430-439.

[12] J. B. Keller and S. I. Rubinow. Asymptotic solutions of eigenvalue problems. Annals of Physics **9** (1960), 24-75.

[13] G. Lamé. Mémoire sur la propagation de la chaleur dans les polyèdres. Journal de l'École Polytechnique **22** (1833), 194-251.

[14] C. Léna. Courant-sharp eigenvalues of a two-dimensional torus. arXiv:1501.02558.

[15] B.J. McCartin. Laplacian eigenstructure of the equilateral triangle. Hikari Ltd 2011. `http://www.m-hikari.com/mccartin-3.pdf`

[16] M.A. Pinsky. The eigenvalues of an equilateral triangle. SIAM J. Math. Anal. **11** (1980), 819-827.

[17] M.A. Pinsky. Completeness of the eigenfunctions of the equilateral triangle. SIAM J. Math. Anal. **16** (1985), 848-851.

[18] Å. Pleijel. Remarks on Courant's nodal theorem. Comm. Pure. Appl. Math. **9** (1956), 543-550.

[19] A. Stern. Bemerkungen über asymptotisches Verhalten von Eigenwerten und Eigenfunktionen. Inaugural-Dissertation zur Erlangung der Doktorwürde der Hohen Mathematisch-Naturwissenschaftlichen Fakultät der Georg August-Universität zu Göttingen (30 Juli 1924). Druck der Dieterichschen Univertisäts-Buchdruckerei (W. Fr. Kaestner). Göttingen, 1925.